Landscape evolution and ice-sheet behaviour in a semi-arid polar environment: James Ross Island, NE Antarctic Peninsula

BETHAN J. DAVIES[1]*, NEIL F. GLASSER[1], JONATHAN L. CARRIVICK[2], MICHAEL J. HAMBREY[1], JOHN L. SMELLIE[3] & DANIEL NÝVLT[3]

[1]*Institute of Geography and Earth Sciences, Aberystwyth University, Aberystwyth SY23 3DB, UK.*

[2]*School of Geography, University of Leeds, Leeds LS2 9JT, UK.*

[3]*Czech Geological Survey, Brno Branch, Leitnerova 22, 658 69 Brno, Czechia.*

[3]*Department of Geology, University of Leicester, University Road, Leicester LE1 7RH, UK.*

**Corresponding author (email: bdd@aber.ac.uk)*

Authors' Note: This pre-print version is the accepted version of the published manuscript, but there are some small changes between this version and the final published version. Please view the final published version here: http://sp.lyellcollection.org/content/early/2013/04/12/SP381.1.abstract

Final citation:

Davies, B. J., Glasser, N. F., Carrivick, J. L., Hambrey, M. J., Smellie, J. L., and Nývlt, D. (2013). Landscape evolution and ice-sheet behaviour in a semi-arid polar environment: James Ross Island, NE Antarctic Peninsula. In "*Antarctic Palaeoenvironments and Earth Surface Processes*." (Hambrey, M. J., Barker, P. F., Barrett, P. J., Bowman, V. C., Davies, B. J., Smellie, J. L., and Tranter, M., Eds.), pp. 1-43. Geological Society of London, Special Publications, volume 381, London.

Abstract: This study of landscape evolution presents both new modern and palaeo process-landform data, and analyses the behaviour of the Antarctic Peninsula Ice Sheet through the Last Glacial Maximum (LGM), the Holocene and to the present day. Six sediment-landform assemblages are described and interpreted for Ulu Peninsula, James Ross Island, northeast Antarctic Peninsula: 1) the glacier ice and snow assemblage. 2) The glacigenic assemblage, which relates to LGM sediments and comprises both erratic-poor and erratic-rich drift, deposited by cold-based and wet based ice and ice streams respectively. 3) The boulder train assemblage, deposited during a mid-Holocene glacier readvance. 4) The ice-cored moraine assemblage, found in front of small cirque glaciers. 5) The paraglacial assemblage includes scree, pebble-boulder lags, and littoral and fluvial processes. 6) The periglacial assemblage includes rock glaciers, protalus ramparts, block fields, solifluction lobes and extensive patterned ground. The interplay between glacial, paraglacial and periglacial processes in this semi-arid polar environment is important in understanding polygenetic landforms. Crucially, cold-based ice was capable of sediment and landform genesis and modification. This landsystem model can aid the interpretation of past environments, but also provides new data to aid the reconstruction of the last ice sheet to overrun James Ross Island.

Polar deserts were widespread during the Pleistocene (in high-latitude continental interiors) and are common today, both in the Arctic (e.g. Svalbard, Canadian High Arctic) and the Antarctic (e.g. Vestfold Hills, Dry Valleys; Alexander Island). However, geomorphological processes are poorly understood within polar deserts despite their widespread occurrence. In particular, the interrelationship of geomorphological (such as cold-based and warm-based glacial, periglacial and paraglacial) processes in polar deserts has been the subject of relatively few papers (Fitzsimons 2003; Haeberli 2005; Waller *et al.* 2009). This paucity of data and information is surprising because geomorphological processes within polar deserts provide information on past and present ice sheet and glacier dynamics and stability, mass and contribution to sea level rise (Waller 2001; Kleman & Glasser 2007).

Landsystems use modern analogues to understand geomorphological processes and process-form relationships through the characterisation of terrain with repeated patterns in surface form and sediments (e.g., Evans & Twigg 2002; Evans 2003b; Benn & Lukas 2006; Golledge 2007; Hambrey & Fitzsimons 2010). When constrained by detailed modern analogues, large scale geomorphological mapping and a landsystem approach can provide proxy data for palaeo-glaciological models and palaeoclimatic reconstructions (Evans 2011). Landsystem models have been presented, among others, for cold-based glaciers in East Antarctica (French & Guglielmin 1999; Fitzsimons 2003; Hall & Denton 2005), glaciated Alpine valleys (Spedding & Evans 2002), active temperate ice sheets (Evans & Twigg 2002; Evans 2003a) and polythermal glaciers (Glasser & Hambrey 2003), but an original model has yet to be developed for a semi-arid polar desert.

Palaeo-ice sheet reconstructions require a thorough understanding of current and past processes and subglacial conditions. Existing reconstructions of Antarctic Peninsula Ice Sheet extent, character and behaviour rely on poorly dated and sparse marine-dominated geological evidence (Heroy & Anderson 2005; 2007; Davies *et al.,* 2011), and there have been few detailed terrestrial studies (e.g., Ingólfsson *et al.* 1992; Hjort *et al.* 1997; 2003; Johnson *et al*. 2011). The relatively accessible Ulu Peninsula on James Ross Island (Fig. 1) is one of the largest ice-free regions in the Antarctic Peninsula, and therefore provides an ideal opportunity to investigate palaeo- and modern geomorphological and sedimentary processes. Previous studies on James Ross Island have focussed on only small individual landforms (e.g., Chinn & Dillon 1987; Rabassa 1987; Lundqvist *et al.* 1995; Strelin & Sone 1998; Fukui *et al.* 2007; 2008), and there is a need for a larger scale, holistic study. Furthermore, the higher precipitation rate and relatively northern latitude of James Ross Island means that meltwater is more readily available than, for example, the Dry Valleys of East Antarctica, making this a different landsystem that requires a new conceptual model. The aims of this paper are to provide a modern analogue to aid the interpretation and understanding of ancient polar deserts, and through interrogation of this to present new data regarding the character and behaviour of the Antarctic Peninsula Ice Sheet through the Last Glacial Maximum (LGM) and Holocene Epoch on James Ross Island.

Study Area

Location and climate

James Ross Island (north-eastern tip of the Antarctic Peninsula; Fig. 1) has a cold, polar-continental climate (Martin & Peel 1978), influenced by the orographic barrier of the Trinity Peninsula mountains (Domack *et al.* 2003; King *et al.* 2003; Davies *et al.* submitted). It is separated from Trinity Peninsula by the 4 – 8 km wide and 450 – 1200 m deep Prince Gustav Channel (British Antarctic Survey 2010). Mean annual air temperatures on Ulu Peninsula are around -7°C (Laska *et al.* 2010, 2011) and can reach up to +8°C in January, with more than 200 positive degree days and 100 freeze-thaw days per year, which are highly variable year-on-year (NASA 2004; Laska *et al.* 2011). Estimates of precipitation range from 200 mm a^{-1} w.e. (water equivalent) (Strelin & Sone 1998) to 500 mm a^{-1} w.e. (van Lipzig *et al.* 2004), which falls into the range of a 'semi-arid' climate (cf. Laity 2008). However, prevailing strong south to south-westerly winds on James Ross Island are effective in encouraging ablation through snow drift. The combination of relatively dry air and high wind speeds exacerbates evaporation and sublimation. Ice and snow melt and ground ice thaw is restricted to the short summer season and varies strongly diurnally in response to cooler night time temperatures and a low angle of incidence of the sun.

Place names on Ulu Peninsula in this study follow the Czech Geological Survey (2009), the British Antarctic Survey (2010) and the Antarctic Digital Database, with the following important exception: the informal name "Whisky Glacier" for the small land-terminating glacier extending north from Lookalike Peaks (Chinn & Dillon 1987; Laska *et al*. 2010; 2011; Engel *et al.* submitted) is not used (Fig. 2). "Whisky Glacier" has never been formally recognised. It is also known as "IJR-45" in the glacier classification by Rabassa *et al.* (1982) (also Hjort *et al.* 1997; Davies *et al.* submitted). Subsequently, the much larger tidewater glacier draining Dobson Dome into Whisky Bay was officially designated as Whisky Glacier (British Antarctic Survey 2010). Accordingly, we use "IJR-45" when referring to the land-terminating glacier described by Chinn & Dillon (1987). Elsewhere, informal names have been allocated where no formal names exist and are indicated by the use of parentheses (e.g., "Unnamed Glacier"). Finally, although Ulu Peninsula refers to the entire area of land extending between Röhss Bay and Cape Lachman (Fig. 2), our usage generally refers to that part of Ulu Peninsula between Whisky Bay, Cape Lachman and Shrove Cove.

Geological and glaciological history

The Permo-Triassic metamorphic Trinity Peninsula Group crops out widely on Trinity Peninsula (Fig. 1; Barbeau *et al.* 2010). It was intruded by Jurassic and Cretaceous felsic plutons, including granite, granodiorite, quartz monazite, tonalite and gabbro (Bibby 1966; Riley *et al.* 2011; Žák *et al.* 2011). James Ross Island comprises Late Cretaceous sedimentary strata with locally fossiliferous marine sandstone, shale and conglomerate, overlain by the Neogene James Ross Island Volcanic Group (Fig. 1; Bibby 1966; Nelson 1975; Ineson *et al.* 1986; Košler *et al.* 2009; Riley *et al.* 2011). The latter includes tuff, hyaloclastite, basaltic lava and glacigenic diamictite (Pirrie *et al.* 1997; Jonkers *et al.* 2002; Smellie *et al.* 2006; 2008; Nelson *et al.* 2009) and marine laminites (Nývlt *et al*. 2011). The tillites and glaciomarine diamictites contain pelitic metamorphic, altered volcanic and granitic erratics derived from Trinity Peninsula, indicating that the area was inundated on multiple occasions by ice caps during the Neogene (Pirrie et al. 1997; Hambrey & Smellie 2006; Smellie *et al.* 2006; Hambrey *et al.* 2008; Nývlt *et al.* 2011). The basalt lavas form resistant caps on the Cretaceous strata, resulting in flat-topped mountains (mesas) surrounded by scree.

During Quaternary glaciations, James Ross Island was overwhelmed by ice sheets from Trinity Peninsula, which deposited numerous metamorphic and granitic erratics across the island (Bibby 1966; Johnson *et al.* 2011). Glacial drift, drumlins and moraines have been described from the interior of Ulu Peninsula (Rabassa 1983, 1987; Hjort et al. 1997; Strelin *et al.* 2006). Prince Gustav Ice Stream developed during the Last Glacial Maximum (LGM), diverting ice flow north and south around the island (Gilbert *et al.* 2003; Evans *et al.* 2005). This ice stream receded from the shelf edge after 18 ka BP (Heroy & Anderson 2007; Davies *et al.* 2011), with retreat to the inner shelf occuring between 17.5 and 9.1 ka (Johnson *et al.* 2011). Mean exposure ages on granite erratics at Cape Lachman are dated to 8.0 ± 0.8 ka, suggesting recession of the ice stream from northern James Ross Island by that time (Johnson *et al.* 2011). Radiocarbon dates from glaciomarine sediments on The Naze, James Ross Island (Fig. 1) indicate that Herbert Sound became ice free by 6.3 ± 0.3 to 7.8 ± 0.2 cal. ka BP (Hjort *et al.* 1997; calibrated and corrected by Davies *et al.* 2011), and this is supported by recent cosmogenic nuclide exposure ages on erratic boulders from 6.8 ± 0.7 ka from Terrapin Hill. Johnson Mesa maintained a small independent ice dome until 6.6 ± 0.7 ka (Johnson *et al.* 2011).

Several mid-Holocene glacial advances have been documented on James Ross Island. There was an advance of Croft Bay glaciers to Cape Lachman from 7.3-7.0 cal. ka BP (Strelin *et al.* 2006; Johnson *et al.* 2011). A later mid-Holocene readvance of “IJR-45” deposited the very prominent line of hyaloclastite and tillite boulders from the existing margin of “IJR-45” northwards to the southern coastline of Brandy Bay. The large lateral moraine related to this advance and flanking Brandy Bay was radiocarbon dated to between 5.4 and 4.7 cal. ka BP (Hjort *et al.* 1997; recalibrated by Johnson *et al.* 2011), suggesting that this glacier readvance may have coincided with the mid-Holocene collapse of Prince Gustav Ice Shelf (absent from 6 to 2 ka; cf. Pudsey & Evans 2001). Lake cores indicate that the climate was warmer at this time (Björck *et al.* 1996). Prominent ice-cored moraines in front of cirque glaciers also suggest a Late Holocene or Little Ice Age readvance (Carrivick *et al.* submitted).

James Ross Island is now 75 % glacierised, and is dominated by the Mount Haddington Ice Cap. The disintegration of Prince Gustav Ice Shelf in 1995 was associated with rapid recession of tributary glaciers (Glasser *et al.* 2011; Davies *et al.* submitted). Periglacial landforms are today well developed on James Ross

Island and on surrounding islands (Lundqvist *et al.* 1995; Ermolin *et al.* 2002; 2004; Strelin *et al.* 2006; Fukui *et al.* 2008).

Methods

Geomorphological mapping was achieved through visual interpretation of remotely sensed images (Table 1) and through an intensive field campaign that covered 200 km^2 of Ulu Peninsula from January-March 2011. Identification of glacially-associated landforms from remote images is well established (Glasser & Jansson 2005; Glasser *et al.* 2005; 2009a; 2009b). Remotely-sensed structural glaciological mapping followed standard procedures (Hambrey & Dowdeswell 1994; Glasser *et al.* 1998; Hambrey & Lawson 2000; Hambrey *et al.* 2005; Glasser *et al.* 2011). Landforms and sediments and were mapped and logged in the field following procedures outlined in Gale & Hoare (1991), Jones *et al.* (1999) and Evans & Benn (2004). Sediments were characterised and quantitatively differentiated through the collection of 101 samples each of 50 clasts (with an *a*-axis from 4 to 32 mm) from a 50 x 50 cm area. Stone lithologies were identified according to the methods of Bridgland (1986), Gale & Hoare (1991) and Walden (2004). A minimum of 30 basalt pebbles were measured to the nearest 0.5 cm for shape-roundness data, following Benn & Ballantyne (1994). Shape-roundness analysis included calculation of the co-variance of the C_{40} and RA indices (cf. Adam & Knight 2003). The C_{40} index is the percentage of clasts with a *c/a* ratio of ≤ 0.4. The RA index is the percentage of very angular and angular clasts within the sample, using the Powers (1953) roundness chart. Only basalt clasts were used to avoid introducing bias into the dataset through the use of different lithologies. These analyses have resulted in the identification of six genetically-grouped sediment-landform associations (Fig. 2; Table 2), which are described and interpreted sequentially in the next section.

Geomorphology and sedimentology

Glacier ice and snow assemblage

Description. James Ross Island has numerous small cirque, valley, tidewater and plateau dome glaciers (Table 2). Most of these glaciers are receding (Table 3), but the land-terminating cirque glaciers on Ulu Peninsula (Fig. 3) have only small rates of recession or their margins are currently stationary. However, 100-200 m of recession has occurred since the most recent glacial advance, when prominent ice-cored moraines were formed (Carrivick et al., submitted). Volume loss has been observed on Davies Dome and “IJR-45”, of 29.7 % and 10.9% respectively from 1979 to 2006 (Engel *et al.* submitted).

Glacier surfaces are characterised by continuous layering (*sensu* Hambrey *et al.* 2005), that is clearly visible both in the field and in aerial photographs (e.g. Figs 2 and 3). On “IJR-45”, there is well-developed continuous layering down glacier (Fig. 2) and supraglacial debris on either side of the ice divide. “IJR-45” is 150 m thick, with a uniform bed topography (Engel *et al.* submitted) and a large debris-covered terminus (“IJR-45 Glacier Moraine”). No crevasses or crevasse traces were visible on any glaciers on the aerial photographs although crevasse traces were noted on the surface of “Unnamed Glacier” and “IJR-45” during fieldwork. The continuous layering in “Unnamed Glacier” is folded about the flow-parallel axis. Supraglacial scree that falls onto the surface of this glacier at the headwall apparently emerges near the snout (Fig. 3B). Glaciers on the eastern side of Lachman Crags (Fig. 3C) are characteristically small and detached from the plateau ice dome and thus presumably from their accumulation areas. They also have prominent ice-cored moraines. Davies Dome flows radially from the top of a mesa. Its lightly folded continuous layering follows the lobate ice margin. Whisky Glacier is characterised by sparse crevasses, crevasse traces and continuous layering (Fig. 2). Perennial snow banks lie in the lee of hill slopes (Fig. 2), feeding ephemeral streams that flow on positive degree days. These snow banks are sometimes associated with protalus ramparts and nivation hollows.

Interpretation. The continuous layering (e.g. Fig. 3) is interpreted as primary stratification formed through firnification, superimposed ice formation, and melting and refreezing of snow. Folding of primary stratification in “Unnamed Glacier” occurred during down-glacier transport about the flow-parallel axis in a compressive regime (cf. Wadham & Nuttall 2003; Hambrey *et al.* 2005). However, the continuous stratification in marginal areas (and lack of foliation) suggests that ductile deformation and shear is not prevalent on these small cirque glaciers. The lobate planform pattern of stratification on Davies Dome indicates that the ice is flowing radially out of the dome. Crevasse traces on “Unnamed Glacier” and “IJR-45” suggest that these glaciers were more active in the past, and that these are now relict features (cf. Hambrey & Lawson 2000).

The supraglacial debris on the surface of some of these glaciers (e.g. “Unnamed” and Triangular glaciers; Fig. 3B) indicates limited subglacial and supraglacial transport, probably through small-scale creep (Hambrey & Lawson 2000). The small glaciers on the eastern side of Lachman Crags (Fig. 3C) are stagnating and down-wasting *in situ*, presumably because the prevalent south-westerly winds starve them of precipitation. In this location, the abundant scree provided by the basalt and hyaloclastite cliffs provides ample debris, creating ice-cored moraines or rock glaciers (e.g. Strelin *et al.* 2007).

There is little evidence of contemporary thrusting and active moraine formation on these small cirque glaciers today; they are now passively down-wasting and slowly receding, with a negative mass balance (Carrivick *et al.* submitted). The separation of some of these glaciers from their plateau accumulation areas has further encouraged ice stagnation. Despite a climate similar to that in Svalbard, none of these glaciers have structures indicative of past surge behaviour, such as looped moraines, pot holes or distorted longitudinal foliation (cf. Sharp *et al.* 1994; Bennett *et al.* 2000b; Hambrey & Lawson 2000; Murray *et al.* 2000; 2002; Hambrey *et al.* 2005; Kjær *et al.* 2008; Grant *et al.* 2009).

Glacigenic assemblage

Ulu Peninsula is covered with a superficial drift sheet dominated by basalt pebbles and occasional erratics, which together form an armoured surface that overlies sand (Table 4). In some coastal areas the superficial drift is overprinted by marine terraces.

Erratic-poor drift

Description. A basalt pebble-cobble gravel is widespread across Ulu Peninsula and comprises unlithified subangular basalt pebbles and cobbles forming a lag on the surface, with frequent basalt boulders and rare granite boulders (Table 4). Samples from Solorina Valley (Fig. 2) and the foreground of "IJR-45" show that this erratic-poor 'drift sheet' is typically >90 % basalt, and clasts on the surface are angular to subangular. In each case, there are few Trinity Peninsula erratics. These basalt and erratic boulders can be both well-embedded in the surface or rest on top of it (compare Figs 4A and 4B), and are generally faceted and occasionally striated. Stone stripes and polygons are typically well developed on this surface. This 'drift sheet' is prevalent on topographically flat and smooth, relatively featureless parts of the landscape.

The erratic-poor drift comprises two further sub-elements: firstly, an unlithified, poorly-compacted, broken regolith of local Cretaceous siltstone, sandstone and flaggy sandstone slabs, which is frequently scattered with subrounded to subangular erratic basalt cobbles (Table 4). Patterned ground is often well developed, as illustrated in Fig. 4C. Large isolated basalt and occasionally granite cobbles and boulders are present on the otherwise topographically smooth surfaces (Fig. 4D). The second sub-element comprises exposed Cretaceous bedrock with few or no erratics and little surficial regolith, and clearly visible bedding planes (e.g. Fig. 4E).

Interpretation. Drift sheets comprising an unconsolidated sandy boulder gravel with a pebble-cobble armour are regularly observed in deglaciated Antarctic regions, particularly in the Dry Valleys of East Antarctica (Higgins *et al.* 2000; Augustinus 2002; Hall & Denton 2005; Bockheim 2010), where they are inferred to have been deposited by cold-based ice. The climate of the Dry Valleys today (which is colder and drier than that of modern James Ross Island; Fitzsimons 2003) is probably comparable with the LGM climate on James Ross Island. Sediment-landform assemblages observed in the forefields of cold-based glaciers in the Dry Valleys, Antarctica, include striated boulders, sandstone and siltstone breccia, isolated boulders on drift sheets, boulder trains and ice-cored debris cones. Diamicton, silt and clay are typically absent (Waller 2001; Atkins *et* *al.* 2002; Lloyd Davies *et al.* 2009; Hambrey & Fitzsimons 2010). These drift sheets are distinctly different from subglacial till, which is formed by wet-based ice at the ice-bed interface by a combination of sliding, shearing, lodgement and deformation. Subglacial till is characteristically a diamicton with a high bulk density and shear strength, an unlithified, over-consolidated, heterogeneous and unsorted matrix, and normally bearing polished, striated and faceted stones; the diamicton may be massive, fissile, jointed, and may contain numerous inclusions and other sedimentary structures (cf. Evans *et al.* 2006; Benn & Evans 2010).

The cold-based sediment-landform assemblages noted in other parts of Antarctica (e.g., Atkins *et al.* 2002; Lloyd Davies *et al.* 2009; Hambrey & Fitzsimons 2010) are very similar to the erratic-poor drifts on James Ross Island (cf. Table 4). Key similarities include the lack of till, the pebble-cobble armour with occasional striated boulders and the lack of constructional landforms. The smoothed and sculpted surfaces evolved over millennia with repeated warm- and cold-based ice sheets throughout the Cenozoic (Davies *et al*. 2011), and with only very minor modification during LGM cold-based glaciation. This erratic-poor drift is therefore interpreted as having been deposited by a cold-based ice sheet. Basal sliding is likely to be limited to bedrock regions (Cuffey *et al.* 1999; Waller 2001). The relatively soft, poorly consolidated Cretaceous sedimentary strata that underlay the last ice sheet on James Ross Island were likely to have been deformed, encouraging sheet-flow in much the same way as under warm-based ice sheets above the pressure melting point, but at lower speeds (cf. Fitzsimons *et al.* 1999; Cuffey *et al.* 2000; Fitzsimons *et al.* 2008). Based on the extent of these drift sheets and their rare granite erratics, the ice sheet that overwhelmed the island during the LGM was sourced from Trinity Peninsula, during large scale continental-wide glaciation that extended to the shelf edge (Heroy and Anderson 2007). The minimal meltwater produced at the base of cold-based ice minimised entrainment, erosion, transport and deposition, and reduced the ability of the ice sheet to construct moraines and landforms; this resulted in the smooth land surfaces with minimal glacigenic landforms observed on Ulu Peninsula.

The principal surficial sediment lithofacies are differentiated as erratic-rich or erratic-poor on the presence or absence of Trinity Peninsula Group erratics (Fig. 5A). Most samples show considerable modification from scree, which is presumed to supply the majority of the debris. Material is inferred to have been transported via supraglacial and subglacial pathways. Two samples from the erratic-poor drift from Solarina Valley and St. Martha Cove (Fig. 1) have particularly angular clasts, which could reflect intense post-depositional frost shattering.

Erratic-rich drift

Description. In some coastal regions adjacent to Prince Gustav Channel, such as Lewis Hill, San Carlos Point and Cape Lachman (Figs 1, 2), there are drift sheets comprising poorly-compacted, unsorted sandy boulder gravel with high percentages of Trinity Peninsula erratics from pebble to boulder-size (Table 4). At Cape

Lachman, the central neck of the promontory is significantly enriched with erratics (see Figs 2 and 4F). Where the ground rises, there is a sharp contrast with the erratic-poor drift that is almost entirely composed of the James Ross Island Volcanic Group. There are large numbers of granite boulders in the topographically lower neck of the promontory, but none above the lateral margins of the coastal erratic-rich drift. These erratic-rich sediments are associated with constructional ridges and moraine fragments, such as Kaa Bluff (Fig. 4G). Similar erratic-rich drifts also occur in isolated patches in cols and passes of Ulu Peninsula (cf. Fig. 2), such as Baloo Col, San José Pass, Crame Col, Andreassen Point and in St. Martha Cove, where there are a number of small unconsolidated mounds. North of St. Martha Cove, hyaloclastite mounds are streamlined north-south.

Interpretation. During the LGM, Prince Gustav Ice Stream flowed northwards along the north-western coast of James Ross Island (Camerlenghi *et al.* 2001; Gilbert *et al.* 2003; Evans *et al.* 2005) and impinged upon its coastal regions, resulting in lateral moraines and the erratic-rich drift. The sharp boundary between erratic-poor and erratic-rich sandy boulder gravel on Cape Lachman results from an arm of the ice stream flowing over the lower col, perhaps with cold-based ice on the higher parts of the promontory.

Patches of erratic-rich drift also occur in cols and passes (Table 4). However, there is no evidence of ice streaming over these cols and passes (cf. Stokes & Clark, 1999, 2001). Rather, the large accumulations of erratics indicate enhanced deposition and therefore wet-based subglacial conditions. As ice flowed over the cols it became focussed and compressional stresses increased. Pressure melting point was reached, allowing subglacial deposition and resulting in the erratic-rich sandy boulder gravels and further erosion of the cols (Lloyd Davies *et al.* 2009). Both ice deformation and frictional sliding can increase basal temperatures (Waller 2001). Furthermore, overriding escarpments can lead to ice-bed separation, the formation of lee-side cavities, and further entrainment and deposition. These patches of erratic-rich drift are therefore interpreted to be a result of changes in the subglacial thermal regime during LGM glaciation, which can create mosaics of selective erosion and deposition (Hall & Glasser 2003; Kleman & Glasser 2007).

The accumulation of Trinity Peninsula boulders and erratics on San José Pass is therefore a result of wet-based ice flowing over the col, before flowing out of St. Martha Cove and north up Herbert Sound (cf. Fig. 1), depositing rich accumulations of erratics near Green Lake and ultimately on the eastern slopes of Berry Hill (Fig 2.). Fragments of moraine are associated with this land element at St. Martha Cove, further supporting the suggestion that the erratic-rich drift in this location was deposited by wet-based ice, capable of entraining, modifying and depositing subglacial debris. The ice cap that overwhelmed Ulu Peninsula during the LGM was therefore polythermal, with both regions of warm and cold-based ice. These patches of erratic-rich drift are at odds with the traditional view of ice sheet flow, which envisaged 'islands' of cold-based ice, surrounded and enclosed by faster-flowing wet-based ice (Hughes 1981, 1995).

Care must be taken when interpreting numerous erratics as evidence of a warm-based ice sheet, as the Neogene diamictites on James Ross Island contain Trinity Peninsula erratics (cf. Nelson *et al.* 2009; Nývlt *et al*. 2011). For example, at the northern end of Lachman Crags, east of Crame Col, there is an abandoned cirque. Beneath this is a vast accumulation of granite boulders and numerous Trinity Peninsula-derived pebbles and cobbles. However, in the cliffs bounding the cirque there is a thickness of Neogene tillite (Fig. 2), and these erratics are most likely reworked from Neogene sedimentary strata. The same is true for erratic boulders on the coast between Brandy Bay and Cape Lachman.

Boulder train assemblage

Boulder train and glacial drift

Description. This assemblage comprises “IJR-45 Glacier Moraine”, “Brandy Bay Moraine”, and a boulder train and erratic-poor drift between the two (Table 2). A boulder train of large (7 to 10 m b-axis), freestanding hyaloclastite and diamictite boulders (Figs 2 and 4H) stretches from the western side of “IJR-45 Moraine” to a low ridge flanking western Brandy Bay. The surficial sediments associated with the hyaloclastite boulder train are a sandy boulder gravel, characterised by smooth surfaces, subangular to subrounded basalts, with rare granite or basaltic boulders embedded within the sediments or perched on the surface. The surficial sediments are dissected by rivers and lack clear boundaries.

Interpretation. The surficial sediments are lithologically similar to the LGM erratic-poor drift (Tables 2 and 4), and are stratigraphically younger than the coastal erratic-rich drift. The intact large hyaloclastite boulders are likely to have been transported supraglacially by a readvance of IJR-45 during the mid-Holocene (cf. Björck *et al.* 1996; Hjort *et al*. 1997). The hyaloclastite boulders are perched on, rather than lodged in, the surficial sediments. In addition, these boulders are friable and delicate, and unlikely to survive subglacial transport. Recession was rapid with little reworking of these boulders, and no recessional moraines are visible in the landscape. This boulder train was therefore most probably formed by the marginal dumping of supraglacial debris. Rapid (and possibly cold-based) recession may have protected these friable boulders.

"Brandy Bay Moraine"

Description. The ridge bounding the south-western coastline of Brandy Bay (Fig. 2) is approximately 30 m high with a rounded, undulating crest, 3.5 km long, and up to 0.7 km wide. There is a sharp break in slope at its base, and it declines in elevation from east to west (seawards). The surficial sediments are a basalt pebble-cobble pavement lag with a fine silt matrix buried beneath the cobble armour. There are rare granite boulders, increasing in number seawards. The clast shape-roundness data shows considerably rounder, blockier pebbles than the ice-cored moraines (Fig. 5B). The percentage of subrounded to rounded pebbles increases northwards along the crest of the moraine. Hyaloclastite boulders decrease in size, and degradation and weathering increase south-eastwards down the crest of the moraine. Adjacent to the ridge near Phormidium Lake, the glacial drift has abundant Trinity Peninsula erratics, contrasting with the surficial sediments on the moraine (see Fig. 2).

On the crest of the ridge are numerous low surface depressions with arcuate scars, 0.5 to 1 m high. Slump scars, debris flows and stone polygons characterise the surface of the moraine. For example, a slump in the slope facing Brandy Bay is more than 7 m wide with a 40 m run-out, and an arcuate headwall scar. This slump has abrupt lateral margins, visible failure planes and desiccated edges. Slumping at the base of the seaward terminus of the moraine resulted in a natural exposure. At the base of the exposed section 0.6 m of stratified dark blue ice with large coarse crystals is present, and contains occasional coarse gravel clasts. It is overlain by 0.5 m of silty clast-rich diamicton that grades into 1.4 m of crudely bedded sand. From 1.9 to 3.3 m in the section, there is a diamicton with a gradually increasing gravel content, overlain by crudely bedded sand.

Interpretation. The ridge in Brandy Bay has previously been interpreted as a moraine (Hjort et al. 1997), and in our study, it is called "Brandy Bay Moraine". The moraine and associated “Bahiá Bonita Drift” were deposited by a readvance of “IJR-45” (Rabassa 1983, 1987; Ingólfsson & Hjort 2002). The readvance has been dated to the Mid-Holocene by radiocarbon dates from marine molluscs in overridden glaciomarine sediments at the base of the moraine, bordering Prince Gustav Channel (Hjort *et al.* 1997), and radiocarbon dates from lake sediments in the boulder train (Björck et al., 1996). Drumlins have been reported in association with the moraine and boulder train (Rabassa 1987; Hjort et al., 1997). However, our fieldwork indicates that these “drumlins” are simply remnants of a thicker Mid-Holocene drift sheet, subsequently dissected by ephemeral streams and reduced by periglacial slope processes.

The basaltic debris on the moraine was derived from reworking of basalt scree and hyaloclastite boulders from Lookalike Peaks and Smellie Peak, which were also the source for the diamictite and hyaloclastite boulders in the boulder train. The percentage of Trinity Peninsula erratics and numbers of granite boulders increases north-westwards along the crest of the moraine, indicating the reworking by wet-based ice of the pre-existing and underlying coastal erratic-rich drift. Conversely, the hyaloclastite boulders decrease in number and size northwards along the crest of the moraine as a result of increasing degradation and *in situ* weathering.

Subglacial transport is suggested by the clast shape-roundness data (Fig. 5), with considerably less angular material than the ice-cored moraines and the basalt-rich drift. This glacier advance was synchronous with the recession of ice from Johnson Mesa and the collapse of Prince Gustav Ice Shelf (Pudsey & Evans 2001;

Johnson *et al.* 2011), suggesting a warmer climate. This is supported by evidence from lake cores (Björck *et al.* 1996). However, constraints on radiocarbon dating limit our ability to refine the timing of these events. The moraine remains ice-cored at depth because of its large size and thick debris cover (which is considerably thicker than the active permafrost layer of 1 m and thus protects the ice core from further melting), and this ice is genetically related to the abundant permafrost features found on its crest. The large thickness of sediment cover is sufficient to protect the ice core from further ablation.

"IJR-45" currently has only a small accumulation area. For the creation of such a large moraine, coalescent glaciers with accumulation areas on Lachman Crags, Davies Dome and Johnson Mesa must be invoked. In addition, shifting ice divides may have favoured "IJR-45" over Alpha Glacier, resulting in glacier advance. The survival of delicate hyaloclastite boulders in the boulder train suggests that detachment from its accumulation area during the mid-Holocene resulted in rapid recession.

"IJR-45 Glacier Moraine"

*Description. "*IJR-45 Glacier Moraine" is up to 1 km wide, with low slope angles until the edge of the moraine, where it drops off sharply (Fig. 6A). The glacier trunk comprises clean ice and ice with a thin debris cover. The lateral-frontal complex comprises a chaotic assemblage of small, sharp-crested ridges 1 to 3 m high and up to 1 m wide and lines of boulders. Stratified ice is frequently exposed in back scars in this location. However, the region of intensely ice-cored moraine only extends for 50 m from the glacier snout. In this frontal region, the surficial sediments are highly variable, with localised patches of fossiliferous sandstone, mudstone and diamicton amongst the largely hyaloclastite-derived basalt sandy boulder gravel. In the immediate ice frontal region, the abundant meltwater mixes with fines to produces muddy, clast-rich diamictons. Glacier ice is inferred to continue westwards beneath the high frontal-lateral moraines (Engel *et al.* submitted).

The next 50-160 m from "IJR-45" snout are characterised by increasingly degraded down-wasting back scars with exposed stratified blue and white ice, small sharp-crested ridges 1-3 m high, and numerous small perched lakes. The ridges follow the arcuate form of the primary stratification in the glacier ice, and are often asymmetric, with steep stoss faces and gentle lee faces. There is abundant meltwater dissecting the moraine-mound complex. The ice exposed in a back scar close to the snout ("IJR-45 4"; see Fig. 6A for location) has 5 m of bubble-poor, large, dark blue and well-defined ice crystals 0.05-0.10 m long, overlain by 0.50 m of sediment.

From 160-400 m back from the glacier snout, there are subdued crescent-shaped scars, circular niches and ridges with no ice visible, and numerous large hyaloclastite boulders, down-wasting and weathering *in situ*. The moraine surface is characterised by a pebble-boulder lag of subangular to angular basalts. There is a large frozen lake (> 100 m diameter) and numerous small perched lakes, as well as several circular depressions from drained lakes.

From 400-1000 m back from the glacier snout, on the glacier true left-lateral moraine, the ridges widen and flatten down-slope into a 100 m wide ridge, sometimes with small 5 m high subsidiary ridges and isolated mounds. The ridges become increasingly subdued with distance from the ice margin. In this lateral position, stone stripes and patterned ground are clearly developing. There are no ice scars, although there are numerous ridges topped with lines of hyaloclastite boulders that reflect the orientation of the primary stratification in the glacier ice (Fig. 6A). These hyaloclastite boulders are up to 7 m in diameter. The moraine surface texture varies spatially, with areas of striated, faceted boulders, and areas with subangular to angular basalts showing little sign of glacial transport. There are rare small lakes. The true right-lateral moraine is similar. For example, "IJR-45 5" is characterised by a flattened ridge, 100 m wide, scattered boulders and isolated mounds and periglacial polygons. In regions more distal to the terminus, there is a basalt-rich boulder gravel with a coarse orange sand matrix, derived from the *in situ* weathering of massive hyaloclastite boulders.

From 1000 m from the glacier terminus to the upslope limit of the visible moraine, the moraine is characterised by smooth slopes with loose scree, frost-shattered basalt boulders, well-developed periglacial stone nets and stripes, drained lakes, and subdued ridges. There are large numbers of hyaloclastite boulders, particularly to the true left of the moraine, and subdued arcuate ridges. The outer face of the moraine is steep, lobate, and contrasts sharply with the glacial drift in the forefield (the photograph Fig. 4B was taken in front of "IJR-45", which is visible in the distance). On the western flank of Smellie Peak, adjacent to the moraine terminus, a stream has incised a steep 10 m-deep channel. A series of three small, dry tributaries join this stream, running consecutively across the steep slope and at an angle to the fall line.

Interpretation. "IJR-45 Glacier Moraine" is characterised by five different zones (Table 5 and Fig. 6B and 6C). Fresh, actively back-wasting ice scars in the frontal-lateral complex grade outwards to increasingly smoother slopes, more uniform and compacted sediments, and increasing weathering and disintegration of hyaloclastite boulders. "IJR-45 Glacier Moraine" is separated from the ice-cored moraines of the Late Holocene Assemblage because of its older age, deduced on morphostratigraphical grounds, such as advanced periglaciation and ice-core degradation.

Zone 1 comprises clean glacier ice and glacier ice with a thin debris cover. The moraine near the snout of "IJR-45" (Zones 2-3) has many features typical of ice-cored moraines formed through the thrusting of polythermal ice at the glacier margin (summarised in Table 5), including stratified, inclined glacier ice, ice scars, perched ponds, steep slopes, ridges and scarps (e.g., Østrem 1964; Knight *et al.* 2000; Schomacker & Kjær 2007). Sediment accumulates through the meltout of thrusted subglacial sediments, englacial debris bands, and channel-fill materials. Supraglacial material is also a significant component of the debris mantling the glacier surface. De-icing processes include backwasting and downwasting (cf. Krüger *et al.* 2010). This causes surface lowering and flattening of ice-cored slopes. Collapse results in the breaking of sediment cover and the exposure of new ice walls and new cycles of ice degradation. Resedimentation occurs through slumping, sliding and sediment flows, and reworking from fluvial, aeolian and periglacial (freeze-thaw) action. The occasional striated boulders indicate active subglacial transport. This zone may have been contemporaneous with the Late Holocene assemblage.

Zones 3 to 5 are typical of dead-ice (stagnant glacier ice) environments (cf. Krüger *et al.* 2010), where melting of buried ice results in resedimentation processes (Bennett *et al.* 2000a). This is dead-ice-cored moraine, with large volumes of supraglacial, englacial and subglacially transported debris (cf. Klint *et al.* 2011). Water allows liquefaction and reduces the shear strength of the sediment, encouraging further mass movement. The large depth of sediment cover in the dead-ice-cored and permafrost zones protect the ice from further ablation. Indeed, once the accumulated sediment on the moraine becomes thicker than the active layer, estimated to be 1 m (Ermolin *et al.* 2002; 2004), the ice core is preserved. There is little sign of active ice melt in zones 4 and 5, illustrating the nature of dead-ice terrain (Klint *et al.* 2011). Landforms of this type are typical in polar arid environments in East Antarctica (Fitzsimons 2003), Svalbard (Lønne & Lyså 2005; Lukas *et al.* 2007; Jacobs *et al.* 2011) and Iceland (Kjær & Krüger 2001; Krüger *et al.* 2010).

“IJR-45 Glacier Moraine” is interpreted as an ice-cored moraine rather than a rock glacier (cf. Chinn & Dillon 1987) because of limited evidence for downslope movement, the lack of a continuous supply of talus, and the evidence of thrusting (such as long, arcuate, asymmetric ridges, often with exposed scars of glacial ice, and linear trains of bouldery debris; cf. Hambrey & Huddart 1995; Hambrey et al. 1997) from polythermal glacial processes. The ridges on the outer moraine show former ice position, and are not furrows and ridges related to downslope movement. The distribution of large hyaloclastite boulders across the moraine reflects ice flow, as they are derived from Lookalike Peaks to the southwest of the glacier headwall, and are distributed across the true glacier left. Rather, “IJR-45 Glacier Moraine” is interpreted as a coherent body of stagnant glacier ice, down-wasting *in situ* and overlain by debris.

The landform succession reflects the age and increasing degradation of the moraine, with three stages of landform succession: an initial, dynamic, young phase, with thrusting and upwards ice movement transporting debris to the surface (Zones 1-2); a mature phase of ice-disintegration and sediment reworking (Zones 3-4); and a final or old phase of partially ice-cored terrain (Zone 5). The presence of well-developed periglacial features on “IJR-45 Glacier Moraine” suggests that zones 4 and 5 formed some time ago, and that this dead-ice feature has been slowly degrading for centuries and possibly millennia. The ridges and lobate margin of “IJR-45 Glacier Moraine” (Fig. 6A) suggest that until IJR-45 began to stagnate and down waste *in situ*, it was an active piedmont glacier, expanding out of the valley.

The clast roundness on “IJR-45 Glacier Moraine” is difficult to interpret, as the majority of the basalt clasts are derived from *in situ* weathering of large hyaloclastite boulders. However, they are largely more angular than those clasts on “Brandy Bay Moraine”. The tuff from these boulders also provides the majority of the sand fraction on the moraine. Clasts on the lateral moraine are more angular than those on the terminal moraine. The amount of frost-shattering towards the distal margins of the moraine increases the tendency towards angularity (Fig. 5B). Large basalt screes on Smellie Peak abut the true right moraine of the glacier, and probably represent a major source of clasts. Cretaceous sandstones occur in limited locations in the moraine, reflecting localised bedrock outcrops and low transport distances. The presence of more fines (from Cretaceous sandstone and siltstone) exerts a strong control on moraine character, with patchy outcrops of diamicton and deformed muds in “IJR-45 Glacier Moraine”. Dry channels in front of the moraine may be palaeo-meltwater channels, recording the recession of the glacier up the valley.

Ice-cored moraine assemblage

Description. Ice-cored moraines in front of cirque glaciers and abandoned cirques are amongst the youngest landforms on Ulu Peninsula (Rabassa 1987), and date from a readvance of the small cirque glaciers that was most likely in the Late Holocene (Carrivick *et al.* submitted). The cirques are characterised by steep bedrock headwall cliffs and a rounded, over-deepened basin, and they are occupied by small glaciers or occasionally lakes (e.g. by Davies Dome and the western face of Lachman Crags or the north-eastern slopes of Johnson Mesa). The ice-cored moraines (e.g. Fig. 3) typically have multiple sharp-crested ridges and numerous small lakes and ponds (Fig. 7A, B, C). The surfaces of the moraines range from sandy boulder gravel, through unsorted openwork basalt boulders to diamicton. Pebbles and cobbles are subangular to subrounded and show increasing roundness of shape with proximity to the glacier snout. Exposures reveal stratified glacier ice (layered blue or white ice, bubble poor or bubble rich) that is exposed in ice scars (Fig. 7D, E), and superficial slumps and debris flows. The exposed ice has a fine crystal structure and a low bubble content, and contains debris ranging from sand and fine gravel to small boulders. In San José Glacier moraine, an exposure of ice with stratification dipping at 40° up ice reveals clean blue bubble-free ice, interbedded with white bubble-rich ice, diamicton, fine to boulder-sized clasts and muddy laminations (Carrivick *et al.* submitted). On the terminal moraines there are occasional striated boulders in the terminal moraines (e.g. Fig. 7I).

Clast lithological data gathered from San José Glacier moraine shows that the predominant lithology is the James Ross Island Volcanic Group (Fig. 8A). These basaltic rocks are well exposed in the bedrock cliffs and on the mesa above the glacier. Transport distances, especially for the friable and non-durable Cretaceous sandstone, are very low, with Cretaceous rocks occurring only in specific locations close to their outcrops. Unlike the smoothed glacial surfaces outside the moraines, no Antarctic Peninsula erratics were observed.

The presence of Cretaceous lithologies, especially mudstone, significantly alters the composition of the moraine, with far higher percentages of fines and muds observed. This results in patches of diamicton amongst the largely sandy boulder-gravel of the moraines.

Clast-roundness histograms from gravel-sized basalt clasts vary with sample location. In Lachman and San José glaciers, for example, there is a trend towards increasing angularity of gravel clasts towards the headwalls of the glacier (Fig. 8B). However, this trend is disrupted on the outermost edges of Lachman Glacier moraine, where there are increasing percentages of very angular clasts (Fig. 5). In "Unnamed Glacier" moraine, sample Unnamed 3 has high percentages of angular clasts despite being located in a terminal moraine position. However, there is considerable inter-moraine variability. In general, the ice-cored moraine clasts show more angularity than the older glacial drifts (Figs 5A, B).

The moraines around the Davies Dome plateau glacier (Fig. 7G, H) are texturally and morphologically highly variable. For example, on top of the mesa, where the ice margin is rounded in both planform and surface slope, there is no evidence of landform construction. The lobed south-eastern margin comprises regions of angular unsorted gravel, diamicton ridges, and ridges of angular, frost-shattered basalt. At sample location DD2 (234 m a.s.l.; Fig. 8D), there are small, sharp-crested ridges up to 20 m high and 1 m wide, transverse to ice flow. There are back scars with exposed stratified ice. The proportion of sandstone in the clast count and matrix is highly variable. Mud content varies considerably over small distances, clearly dependent on local bedrock geology, i.e. the presence of Cretaceous deposits. Adjacent to these moraines, ice-contact scree is formed below an ice-cliff, forming angular open-work basalt cobbles and boulders, such as Sample DD1 (217 m a.s.l.), which was taken in front of an ice cliff (Fig. 8). The stratified and dipping ice has a structural unconformity with a layer of angular basalt boulders and cobbles.

Lateral moraines on the outlet glacier, which coalesces with Whisky Glacier in Whisky Bay, are also typical ice-cored moraines. Sample Davies 1 (Fig. 8D) is characterised by a series of small, sharp-crested ridges, 2-20 m high, with basalt boulders perched on their crests. Ice scars expose stratified ice, dipping at 80-90°, with 5-30 cm thick layers of dark blue, bubble-poor and white, bubble-rich ice, both with occasional cobbles; 10 cm thick layers of grey mud; and thin mud layers with occasional fine to medium gravel. The ice has a strong unconformity with the 60 cm thick sediment drape above it.

Interpretation. These hummocky ice-cored moraines are assumed to have formed during the last 200 years, when the Antarctic Peninsula experienced a pronounced cooling event, approximately synchronous with the Northern Hemisphere Little Ice Age (Bertler *et al.* 2011). The moraines are principally composed of stratified ice. Ice with dispersed debris is interpreted as ice from above the basal zone. Ice with laminated debris is formed through the attenuation of debris through creep. The ice with stratified debris is interpreted as being derived from basal adfreezing (Hubbard & Sharp 1995; Knight *et al.* 2000; Waller *et al.* 2000; Hubbard *et al.* 2009).

The debris on the surface of the moraines is composed almost entirely of basalt (cf. Fig. 8A, C), originating principally from rockfall from the headwalls onto the glacier surface. However, sand and mud derived from subglacial reworking of Cretaceous sandstone is evident in the fine-grained matrix in particular areas of the lateral moraines. However, as transport distances of Cretaceous lithologies are low, sandstone gravel forms only a minor component of the moraine lithologies. Subglacially transported debris (such as striated boulders) is apparent, particularly in the terminal moraines. Moraine surface character and matrix content are therefore closely controlled by the bedrock geology, with patches of purely basaltic boulder-cobble gravel and diamicton occurring in close proximity to one another.

Ice-cored moraines are formed by the release of material from proglacial or englacial thrusts, melt-out, and supraglacial debris (Glasser & Hambrey 2003; Schomacker 2008; Schomacker & Kjær 2008). Subglacial thrusting entrains sediment, with moraines forming through the thrusting upwards of basal glacial ice at the ice margin, induced through marginal shear. This behaviour is typical of small polythermal glaciers (Hambrey *et al.* 1999; Glasser & Hambrey 2003). Folding, thrusting and stacking of basal ice because of longitudinally compressive flow in polythermal glaciers (where the margin is frozen to the bed) results in the development of moraine ridges with intercalated debris-rich and debris-poor stratification (Boulton 1972; Evans 2009). The angle of thrusting controls not only the angle of moraine slope, but also moraine height, width and character. These are *controlled moraines* (Ó Cofaigh *et al.* 2003; Evans 2009), where the linearity of the moraine is controlled by primary stratification in the glacier ice (e.g. Figs 3, 6 and 8). These moraines indicate that the glaciers were previously more active in the past, with at least temperate ice regime in the snout, which is a common phenomenon in small modern glaciers in the High Arctic (e.g., Hambrey *et al.* 2005; Rippin et al. 2011).

The complexity and variation in moraine around Davies Dome (ice-cored moraines composed of sandy boulder gravel and diamicton; ice-contact scree; flat and featureless on the mesa plateau; Fig. 8D) is likely to reflect variations in thermal regime. Structural glaciological analysis demonstrates that the lobes and outlet glaciers are likely to be polythermal, with a frozen margin, resulting in the formation of ice-cored moraines. Ice-contact scree forms below ice cliffs, where meltout and sublimation results in the deposition of angular englacial and supraglacial debris. The formation of ice-contact scree suggests that the ice margin is stable, and this is a common landform in cold-based glaciers (Fitzsimons 2003). The smooth, flat margin on top of the mesa suggests that this part of the dome is fully cold-based, with little or no movement or modification of the landscape.

The shape-roundness data show some difference between samples from the high lateral moraines and samples from the distal terminal moraines within the same moraine (Fig. 5), although short transport distances mean that these differences are subtle. Samples from the terminal moraines clearly have blockier shapes and edge-rounded corners, which is indicative of subglacial transport. Samples from the lateral moraines are more angular, with less blocky clast shapes. This is indicative of shorter transport distances, and a higher input of supraglacially-derived material. This trend reflects the influence of transport distance on the shape of gravel clasts, and that these small cold to wet-based glaciers are locally capable of modifying their bedload. Angularity again increases towards the older, outer portions of the moraine, as post-depositional frost-shattering fragments basalt clasts. This difference is clearly shown in the C_{40}/RA plot in Fig. 8C, with two distinct populations. However, there is considerable variation between the moraines; this is likely to be as a result of variations in the input material (scree), which is dependent on its origin (refer to Paraglacial assemblage). Also of note is the increase in angularity in some moraines on the distal parts of the moraine. This is likely to be the result of increased frost-shattering in the older parts of the moraine, and thus the older age of their deposition.

Part of the complexity in clast shape is highlighted in “Unnamed Glacier” (Figs 2, 3C). Sample “Unnamed 3” (Fig. 5B) is directly below steep cliffs from which scree is constantly falling onto the glacier surface. This scree is lightly buried by snow, and then observed melting out near the terminus; sample "Unnamed 3”, although from the terminal moraine, is therefore largely derived from supraglacial material that has undergone little modification. This contrasts with “Unnamed 4”, also from a terminal position on the moraine (Fig. 5C), but from a position away from supraglacially-transported material. The edge-rounding of clasts in this location is indicative of subglacial transport.

Post-depositional processes play a key part in moraine development, with aeolian deflation rapidly removing fines, resulting in a lag of cobbles and pebbles on the surface of the moraine. Melting of the ice-core provides abundant meltwater, resulting in numerous debris flows, especially in regions rich in matrix material. Preferential melting of ice core also results in the formation of ice-collapse pits, which subsequently become perched ponds (kettles). With only a thin sedimentary covering, these moraines are particularly prominent only because of the presence of this ice. After ice-core melt out, there will be little geomorphological expression, which explains the lack of other prominent moraines from previous readvances on Ulu Peninsula. Following the terminology of Clayton (1964) and Kjær and Krüger (2001), these are mature, fully ice-cored moraines, characterised by mass movement and resedimentation processes. They can be compared with “IJR-45 Glacier Moraine” and “Brandy Bay Moraine”, which are in an older phase and are classified as “partially ice-cored terrain”.

Paraglacial assemblage

The 'paraglacial period' refers to the period of readjustment from glacial to nonglacial conditions, with the reworking and relaxation of glacial landforms and sediments, such as steep debris-mantled slopes, cliffs and large fluvial systems (Fitzsimons 1996; Ballantyne 2002). Mass-wasting of rock walls, movement on debris-mantled slopes, aeolian processes and limited fluvial transportation dominate sediment transfers, which are limited to the short summer season on James Ross Island. On Ulu Peninsula, paraglacial sediments and landforms overprint older glacial landforms, and paraglacial processes actively modify landforms and transport material.

Marine Terraces and raised beaches

Description. Below 30 m on the Abernethy Flats there are smooth, flat slopes, an absence of large boulders, and rounded pebbles. Shape-roundness Sample Aber 3, at 30 m a.s.l. on the Abernethy Flats (Fig. 9A), illustrates the high degree of rounding on the clasts, with spherical shapes (Fig. 5A). Sample Aber 1 was taken further away from the coastline but still at 30 m a.s.l. It has 18 % angular pebbles, thereby possibly reflecting frost shattering. In this aspect Sample Aber 1 bears a closer resemblance to sample Aber 2, taken from the basalt cobble-gravel glacial drift. The surface near sample Aber 3 is flat and smooth with a deflated pebble-cobble gravel. There are sparsely distributed hyaloclastite boulders.

A series of flat terraces with rounded pebbles were observed near the sea shore in front of Alpha Glacier (Figs 9B and 9C). The uppermost bench, at 7 m a.s.l., has relatively few rounded pebbles. The surface is composed of a sorted basalt pebble-gravel, with no large boulders and a sandy silt matrix. The middle bench (2 m a.s.l.) is separated from the others by steep slopes with active solifluction lobes. This bench dips gently seaward. Frost shattering of pebbles is evident.

Interpretation. Associated with and overprinting the glacial drifts in coastal areas on James Ross Island are a series of marine terraces, formed during and after deglaciation. Marine terraces on James Ross Island occur up to a height of 90 m a.s.l., and date from the Pliocene to the Holocene (Rabassa 1983; Strelin & Malagnino 1992; Roberts *et al.* 2011). Hjort *et al*. (1997) recorded a series of strandlines and beach deposits near San Carlos Point, including beach gravels at 16 m, 30 m and 90 m a.s.l. Hjort *et al.* suggested that the 30 m a.s.l. marine limit observed primarily on the Abernethy Flats was associated with deglaciation of Prince Gustav Channel. A 16 m a.s.l. terrace is a mid-Holocene marine level following further terrestrial deglaciation (Ingólfsson *et al.* 1992; Hjort *et al.* 1997).

Spits and modern beaches

Description. Northern James Ross Island is fringed by beaches, occasionally with sandy spits. Spits occur at San Carlos Point (500 m long, 80 m wide), Cape Lachman and St. Martha Cove (900 m long, 300 m wide). Furthermore, over a distance of 1.8 km on the beach west of Mendel Station (Fig. 2), 79 granite, 19 gneiss and 22 pelitic boulders with a *b*-axis > 1 m were observed. Boulders are also noted on the beach east of Mendel station to the tip of Cape Lachman.

Interpretation. The isolated sand and gravel spits formed through the reworking of glacial and fluvial sediments in the littoral zone (Ballantyne 2002). Littoral longshore currents transported formerly deposited glacial and fluvial material alongside the beach. This coastal reworking has also resulted in a large number of boulders, especially of Trinity Peninsula origin, forming a boulder lag on the beaches, which is typical of paraglacial environments (Ballantyne, 2002). Unstable steep slopes behind beaches are subject to solifluction and over-steepening by wave action, further encouraging accumulations of boulders on the beach.

Rivers and streams

Description. Ephemeral incised streams and braided streams on Ulu Peninsula typically have multiple channels with an active river width of up to 100 m, incised stream cuts, small islands, point-bars and longitudinal mid-channel bars (cf. Miall 1977), which shift rapidly in response to widely variable flows (Figs. 2, 9D, E). The braided river draining Alpha Glacier is characterised by rounded, poorly sorted and clast-supported gravel on point bars (cf. Fig. 5A). The braided channel is incised 1 to 2 m, with numerous small channels actively down-cutting. Seal Stream and Monolith Stream (Fig. 2) are associated with the seaward progradation of the outwash plain in Brandy Bay.

Interpretation. Ephemeral rivers and streams on James Ross Island are fed by perennial snowfields and melting glaciers (Fig. 2) and their discharge varies considerably on diurnal, weekly and monthly timescales. On warm days, these ephemeral rivers and streams are capable of winnowing glacial sediments and incising Cretaceous bedrock. Two contrasting fluvial styles occur; the low-discharge, multi-channel, high-sinuosity, braided stream stage, and the high-discharge low-sinuosity stage with one principal channel. In this stage, the whole of the channel belt is flooded.

Aeolian sediments and landforms

Description. Glacial drifts on Ulu Peninsula are frequently covered by a basalt pebble-cobble armour, commonly only one or two clasts thick, with sand beneath. Accumulations of wind-blown sand are frequently found on the surfaces of snowfields, where it can produce aeolian accumulations several metres thick after snowfield decay (Figs 9E, F). Many of the basalt and granite boulders associated with the erratic-poor LGM drift (cf. Table 4) have smooth plano-concave and plano-convex faces (e.g. Fig. 4B) (Knight 2008). Red staining is common on granite boulders in the LGM drifts on Ulu Peninsula (e.g. Fig. 4A).

Interpretation. Aeolian processes are strong and pervasive on Ulu Peninsula. Winnowing of fine particles from surficial deposits is pervasive on James Ross Island, particularly on the flatter regions such as the Abernethy Flats. This winnowing has resulted in a pebble-boulder lag on the surface of glacial drifts. The dry, unvegetated climate of James Ross Island makes it particularly susceptible to aeolian deflation, and strong katabatic winds exacerbate the process. Similar processes have been observed in East Antarctica (French & Guglielmin 1999; Bockheim 2010) and in Iceland, where, over four years, a recently deglaciated surface went from being 30-40 % clast covered to 90 % clast-covered (Boulton & Dent 1974; Ballantyne 2002). Most of the wind-transported material terminates in the sea, or is caught on snow banks. Basalt ventifacts with smooth plano-convex faces are common, which are typical of recently-deglaciated, periglacial terrain, because of the lack of vegetation cover, the presence of large unburied boulders, the availability of sand through glacial abrasion and mechanical frost weathering, and the strong katabatic winds (Knight 2008). In addition to ventifacts, aeroxysts are present on the surface of basalt and tuff boulders, along with other types of aeolian erosional micro-forms (e.g. tafoni) (Fig. 10H).

The red staining on numerous granite boulders is a red desert varnish, enriched in iron, rather than the manganese frequently associated with hot desert environments. Iron oxides are leached out from the internal rock and are deposited as varnish. Granite is particularly prone to the development of a red desert varnish because it is resistant to physical breakdown and contains iron-bearing biotite (Matsuoka 1995). Well-developed desert varnish forms in semi-arid, sheltered areas, away from wind abrasion. Ventifacts and red desert varnishes are both a common feature of ice-free regions of Antarctica (Matsuoka 1995; French & Guglielmin 1999; Hall & Denton 2005; McLeod *et al.* 2008; Bockheim 2010).

Scree slopes

Description. Scree slopes are common beneath the steep Neogene basalt and hyaloclastite cliffs on James Ross Island, and are an important input into moraines, rock glaciers and protalus ramparts. Clast lithological counts prove that the scree is composed entirely of basalt and hyaloclastite. Three shape-roundness samples were taken from modern and active scree slopes (Fig. 5A, B), where they show considerably more angularity than the Glacigenic assemblage drifts but are similar to the lateral moraines in small cirque glaciers. Scree derived from hyaloclastite (NM2) is more rounded, whilst scree from flood basalts (IJR-45 6; BH1) is more angular (Fig. 5C).

Interpretation. The steep cliffs of the James Ross Island Volcanic Group, with vertically-jointed hyaloclastite deltaic deposits, are particularly susceptible to rock weathering and scree slope formation. When deposited, the hyaloclastite lacks a fine binding matrix so it is often only weakly bound by palagonite clay from alteration of original glass (away from any pore-filling zeolite sediment; Johnson & Smellie 2007). After recession of glacier ice after the LGM, stress-release fracturing and subaerial exposure of the cliffs occurred, making them susceptible to freeze-thaw activity in a periglacial climate (Harris 2007). This has resulted in rapid readjustment and the formation of active scree slopes (cf. Ballantyne 2002), which are a key input for rock glaciers and protalus ramparts, and which are continuing to form actively today.

Large scale mass movements

Description. Large-scale mass-movement is evident on Ulu Peninsula where the James Ross Island Volcanic Group rests upon gently inclined poorly consolidated Cretaceous mudstone (Fig. 2). There is a large landslide on the northern foothill just below the col between Johnson Mesa and Bibby Hill (Figs. 10A, B, C). There are many smaller rockfalls and debris flows at the Andreasson Point massif (Fig. 2). In areas affected by large-scale mass movement, volcanic blocks many tens of metres high (representing the full thickness of the local volcanic sequence) and a few hundred metres long, along with smaller fragments, form enormous jumbled heaps, for example, forming the hilly high ground backing onto Andreasson Point. These blocks have detached from the main ice-capped volcanic outcrops nearby (e.g. the Lachman Crags lava-fed delta is the source for the blocks at Andreasson Point). Elsewhere, similar chaotic blocky terrain formed by mass movement sourced in lava-fed deltas is present on the east side of Lachman Crags (Fig. 10C) to the north of Andreasson Point, and forming the hummocky ground between Davies Dome and Lookalike Peaks (surrounding Sekyra Peak), and between Smellie Peak and Dinn Cliffs.

Interpretation. The large-scale mass-movements are probably controlled by gravity acting on steep-fronted brittle rock masses (delta margins) resting on soft ductile substrate (Cretaceous sediments). They are clearly geologically controlled, the upper surface of the Cretaceous mud representing a décollment surface on which the volcanic blocks can slide. Plough structures suggest that the process is still active, as does the presence of a slab of intact delta several hundred metres along the northeast side of Lachman Crags that is down-dropped tens of metres and separated from the main mesa by a snow-filled gap (Fig. 10D). Rates of movement involved in the formation and advection of slabs are not known. Moreover, the formation of the slabs involved in mass movement has not been investigated in detail. However, instability probably occurred after removal of any surrounding ice, or when the deltas were uplifted above sea level, thus removing the hydraulic support from steep delta fronts; this suggests that formation of the large-scale mass movements began soon after uplift and continued during each interglacial, including the Holocene. Sliding may involve initiation along finer-grained (sandy) “bottom set” layers in the lava-fed deltas, or a deep décollment surface lubricated by water in a permafrost environment. It is also conceivable that the underlying weak Cretaceous mudstone (and probably weakly lithified sandstone) can deform under the weight of the deltas, which are individually a few hundred metres thick. The blocks then move downslope with the active layer. Similar landslides have been observed in Scotland, particularly on the Isle of Skye (Ballantyne 1991; Ballantyne *et al.* 1998). However, they are unusual, because these landscape features rely on the uncommon juxtaposition of thick brittle basalt deltas on weak and deformable Cretaceous sedimentary strata. They should therefore not be regarded as ‘typical’ of semi-arid polar landsystems, unless the appropriate lithologies are present.

Periglacial assemblage

Periglacial and paraglacial processes are closely intertwined on James Ross Island. Massive ground ice and glacier ice underlie many of the landforms on James Ross Island, resulting in abundant periglacial processes. There have been several studies investigating permafrost on James Ross Island and surrounding islands. Electrical resistivity studies have suggested that the active layer here is approximately 1 m deep (Fukuda *et al.* 1992; Ermolin *et al.* 2002; 2004). Slightly lower measurements for the active laver (22-93 cm) and important inter-annual variability (2009-2010) were found by using mechanical vertical probing on a transect from the eastern coast of Brandy Bay, over Johnson Mesa and up to Mendel Station, with variation being controlled partly by altitude, substrate and aspect (Engel *et al*. 2010).

Rock Glaciers

Description. Near the south-eastern corner of Lachman Crags, there are six rock glaciers (Fig. 2; 11A, B). Lachman II Rock Glacier is located at the end of an ice-cored moraine, in front of stagnating glacier ice (Strelin & Sone 1998; Strelin *et al.* 2006; 2007). Where the sediment cover in the moraine in front of the glacier reaches 0.60 m deep, it is interpreted as a rock glacier, with ridges and furrows delimiting flow-like features. The rock glacier extends 700 m down-valley and is approximately 500 m wide, with a surface dip to 4-5° in the flow direction. It ends in a steep talus apron of 24-42°. The central part is incised by an ephemeral stream, and conical holes, occasionally occupied by meltwater, occur on the surface of the rock glacier. Exposures of glacier ice are visible in the central channel, in the conical holes, and in the marginal talus (Strelin & Sone 1998). Lachman II Rock Glacier has a mean annual flow velocity of 0.2 metres per year with a travel distance of 400 m from the initiation of the rock glacier, suggesting it is approximately 2000 years old. Lakes on this rock glacier may have previously been the source for glacier lake outburst floods (Sone *et al.* 2007).

The rock glacier beneath Berry Hill (Fig. 11B) is formed below steep hyaloclastite cliffs. It is at a low angle with a steep frontal face (60° slope), and is detached from the cliff face. There are several small arcuate ridges, 1-2 m high, which are moderately sharp-crested, with numerous circular depressions. There are several flat benches. The surface is 100 % basalt and hyaloclastite, with an orange coarse sandy matrix composed of weathered tuff from the hyaloclastite. There are large blocks of hyaloclastite moving downslope.

Interpretation. Rock glaciers are lobate or tongue-shaped landforms comprising a mixture of rock debris and ice, typically with a lobate, furrowed form, ridges, ponds and a steep terminus and sides. They can be effective transporters of material from cliffs. Rock glaciers can be talus-derived (with debris burying snow and forming interstitial ice) or glacier-derived (Humlum 2000; Degenhardt Jr 2009). Glacier-derived rock glaciers form part of a continuum with, and can evolve from, ice-cored moraines (Evans 1993; Ó Cofaigh *et al.* 2003). Distinguishing between ice-cored moraines and glacier-derived rock glaciers can be challenging; however, rock glaciers must move downslope to be classified as such (similar to glaciers) (Østrem 1971), and would therefore normally occur on slopes, where they advance through the internal deformation of ice (see comparison in Table 6). Lachman II Rock Glacier is a glacier-derived rock glacier. Examples of talus-derived rock glaciers can be found west of Andreassen Point (Fig. 11A), below Berry Hill (Fig. 13B) and in Rockfall Valley (Fig. 2).

Protalus ramparts

Protalus ramparts are curved, flat features, found in association with scree and perennial snow banks. They are bounded on their downslope side by a sharp break in slope, where the talus rests at the angle of repose. Numerous protalus ramparts are formed along Johnson Mesa, the western slopes of Lachman Crags (Fig. 11C) and below Davies Dome mesa (Fig. 11D). They form through the rolling of clasts down perennial snow banks, and indicate the presence of periglacial conditions.

Slope Processes

Description. Solifluction lobes are apparent on many moderate to low-gradient debris-mantled slopes on the island (e.g. Figs 2 and 11E), with many boulders on these slopes 'ploughing' into the sediment, with a keel at the downslope edge. Solifluction processes (French 1988) are also active in modifying ice-cored moraines and degraded ice-cored moraines on James Ross Island. This is apparent, for example, on the outer portions of "IJR-45 Glacier Moraine", and has, in conjunction with slumping and slopewash, reduced slope gradients and subdued ridge crests.

Alluvial fans and valley-fills are also important on James Ross Island, with fluvial, snow avalanches, debris flows and solifluction resulting in gentle fan-shaped sediment accumulations in many valleys. Some of the valley fill has subsequently been dissected by rivers and streams, with sorted material being deposited downstream. In the valleys near Alpha Glacier and St. Martha Cove, the region is dominated by large hyaloclastite hill mantled with extensive scree. The valley-fill deposits are bounded by a sharp break in slope. The ground is moist, with strongly-developed patterned ground and limited incision by small snow bank-fed ephemeral streams. These valley-fill deposits are smooth and flat, and dip downslope at very low angles. Rock streams (*sensu* Wilson 2007) were also observed in small valleys, with coarse rock debris and snow accumulating in a linear deposit with a downslope alignment. They typically have a single thread down the valley axis and extend for hundreds of metres, but are typically only a few metres wide.

Interpretation. Periglacial slope processes are controlled by freeze-thaw activity, rock weathering, frost heave and thaw consolidation. The permafrost table inhibits the downward percolation of water, and the melt of segregated ice lenses provides water, which in turn reduces the internal friction and cohesion in the regolith. Frost creep is one of the main components of solifluction, with slow downslope gravitational deformation of slope materials through freeze-thaw activity (Harris 2007). These unvegetated slopes with thick glacial drift are susceptible to erosion by slope failure, debris flows, tributary streams and surface wash, resulting in gullying, slope-foot debris cones and valley floor deposits (Ballantyne 2002). These processes were observed widely on degraded ice-cored moraines, at the base of scree slopes, on slopes mantling hills (e.g. Fig. 11E), and on slopes covered with Cretaceous regolith.

Freeze-thaw sediments and landforms

Description. Evidence for modification of surface sediments by freeze-thaw activity on James Ross Island includes frost-shattered boulders (Fig. 12A), nivation hollows and processes (Fig. 12B), sorted stone polygons and stripes, sometimes vegetated by moss and lichens (Figs 12C and 12D), and surface cracks. The sorted polygons comprise cells of sand and fine to coarse gravel, surrounded by angular coarse gravel and cobbles.

Pattern widths vary between 0.5 and 4 m. Sorted polygons (*sensu* Ballantyne 2007) are particularly prevalent in areas with a large supply of water, such as near streams and snow banks, but also occur on the summits of mesas and on degraded moraines. Stone stripes with alternating coarse and fine sediment are well developed on some slopes. Nivation hollows were frequently observed on Ulu Peninsula, related to small late-lying snow patches, and are usually a few metres square in size. Weathering and downslope transportation of basalt cobbles on Cretaceous sandstones results in striking black stone stripes (Fig. 4C). Patterned ground overprints all of the other land elements on James Ross Island.

Interpretation. Shattered boulders occur through mechanical weathering induced through freezing and thawing under a periglacial environment (Murton 2007). Polygons on the ground surface may form through the development of vertical ice wedges in the ground (Harry 1988). Sorted stone polygons and stone stripes both form through diurnal needle-ice growth, with the former on flat and the latter on inclined surfaces. The diurnal needle-ice freezing and thawing produces creep on inclined surfaces (Ballantyne 2007). Stone stripes may form in combination with seasonal gelifluction and creep through solifluction, resulting in lobes. The presence of patterned ground indicates that the glacigenic deposits on James Ross Island have undergone significant modification since their initial deposition. Networks of cracks have been interpreted as being the product of the fissuring of seasonally frozen ground (Ballantyne 2002)

Late-lying snow is common on James Ross Island, and snow falls throughout the summer season, leading to numerous snow banks and small perennial snow patches. These snow banks feed many of the ephemeral streams and form nivation hollows (Thorn 1988). The close association of patterned ground with streams and snow banks suggests that water may be a limiting factor in the freeze-thaw cycles that form these features. More liquid water is present downslope of snow banks and in moist areas, encouraging ice wedge growth and resulting in more well-developed polygons and stripes.

Mesas and blockfields

Description. The surface of Lachman Crags mesa (400 m a.s.l.) is smooth and flat, but stone stripes and sorted polygon nets occur in most regions. The surficial sediments are almost entirely basalt clasts, with rare, well-embedded, rounded granite boulders. The pebbles are generally edge-rounded with few angular pebbles (Fig. 5A). At the highest point (above 380 m), the sediments form a blockfield of large, angular basalt boulders (Fig. 12E). These boulders are not faceted or striated, and many are sub-vertical as a result of frost upheaval (Fig. 12F).

Johnson Mesa (320 m a.s.l.) is characterised by stone stripes and polygonal nets, with very rare cobbles and boulders of Trinity Peninsula origin. In the highest parts, the surface comprises a blockfield with some boulders turned sub-vertical through frost action. In a col between Bibby Hill and Johnson Mesa, Trinity Peninsula erratics make up 20 % of the clast lithologies. This col has scattered Trinity Peninsula granites and metamorphic boulders, with an *a*-axis of up to 60 cm.

On Davies Dome mesa (370 m a.s.l.), the topography is smooth with gentle undulation. The margins of Davies Dome plateau glacier have little geomorphological expression and moraines are absent. The surface is a sandy boulder gravel with well-developed stone polygons, and is 100 % basalt. Within the polygons, there is coarse, poorly-sorted sand. No Trinity Peninsula erratics were observed on this mesa. Again, above approximately 380 m, the surface comprises a basalt-derived blockfield, with angular, non-faceted and non-striated basalt boulders.

Interpretation. Blockfields are assumed to develop under periglacial conditions on levelled or gently undulating relief, with autochthonous blockfields developing from the *in situ* weathering of bedrock with limited downslope displacement of blocks (Rea 2007; Goodfellow *et al.* 2008; Ballantyne 2010). The blockfields on James Ross Island have developed on the Neogene basalt plateaux (Fig. 2). Vertical frost sorting and patterned ground with sorted polygon nets and stone stripes indicates periglacial frost action. Some authors argue that initial crack formation in blockfields occurred during the warmer climates of the Neogene (cf. Ballantyne 2010). These cracks were then exploited by ice, resulting in frost wedging of bedrock and granular disaggregation under a periglacial climate. However, recent studies have found no evidence of chemical weathering (Goodfellow *et al.* 2008). The Ulu Peninsula blockfields may have been actively forming through frost action throughout the Quaternary (and possibly Neogene), protected by cold-based plateau ice caps during glacials or remaining unglaciated as nunataks above the height of the ice sheet (cf. Goodfellow *et al.* 2008).

The clast size on the blockfields is highly variable. On Lachman Crags mesa, clast size ranges from boulder-size, open-work blockfields, with boulder size being controlled by joint spacing (e.g. Fig. 12E), to sandy boulder-gravels with well-developed stone circles and fine matrix in the interior of the polygons. The pebble fraction has rounded shapes (Fig. 5A), which is not unusual in long-established blockfields (Ballantyne 2010). Edge rounding through granular disaggregation may imply long-term stability of the surface. There is a clear altitudinal control, with coarser, bouldery blockfields only occurring above 380 m.

The presence of granite and Trinity Peninsula cobbles and boulders on the surfaces of some mesas suggests that they might have previously been overridden by glacier ice from Trinity Peninsula. The absence of erratics on Davies Dome mesa, in comparison with Johnson Mesa or Lachman Crags mesa, could be a result of an expansion of Davies Dome, a cold-based ice cap that preserved and protected the blockfield below (cf. Kleman & Glasser 2007) and deflected Antarctic Peninsula ice during the LGM and previous glaciations. An alternative explanation is that the erratics were deposited subaqueously from icebergs derived from

Neogene ice sheets under glaciomarine conditions, and that the plateaux were subsequently uplifted above the height of the Quaternary ice sheets. There is observational support for the latter suggestion. The Lachman Crags lava-fed delta was emplaced in a marine setting whereas that at Davies Dome was englacial (Smellie *et al.* 2008). The erratics are found only on the Lachman Crags delta, on areas of the mesa top underlain by hyaloclastite, i.e. where the overlying lava 'topsets' have been stripped off. The hyaloclastite surface is flat and at a uniform elevation below the adjacent lava outcrop (except where the lavas are down faulted, as on Johnson Mesa), suggesting that the lava cover was removed by marine erosion during the years and decades following emplacement of the delta in the sea (i.e. contemporaneous erosion). If ice was still present in the Peninsula (cf. Smellie *et al.* 2009), icebergs would be able to drift over the stripped-off areas of Lachman Crags delta and deposit erratics. Significantly, the Davies Dome delta has not suffered similar erosion, nor does it have any erratics. The lower col on Johnson Mesa, however, is assumed to be a flow pathway for Quaternary ice sheets, with concentrated flow encouraging deposition of numbers of Trinity Peninsula erratics.

Discussion

Processes of landscape evolution in a semi-arid polar environment

Using the geological, geomorphological and glaciological studies undertaken on James Ross Island, we present a new landsystems model for landscape evolution on James Ross Island (Fig. 13), which will aid the interpretation of past, present and future glacierised and glaciated environments. A key feature of this new model is the multi-temporal approach. Six sediment-landform assemblages were described and interpreted in the above sections (Table 2), and they mark a change from landscape dominance by large-scale glaciation during the LGM, mid- and late-Holocene glacial readvances, and paraglacial and periglacial processes throughout the Holocene and into the present day. The polar-desert landsystem on Ulu Peninsula is strongly controlled by the geology; basalt mesas dominate the landscape, while being underlain by softer Cretaceous marine deposits and a basalt pebble-cobble gravel covers almost all surfaces, and differences between the six identified sediment-landform assemblages are subtle. The large landslides (Fig. 10) are predicated by the presence of basalt deltas, likely to be an uncommon feature of other polar desert environments. However, similar features have been noted elsewhere (e.g., the Isle of Skye, where basalt columns overly Jurassic mudstones (Ballantyne 1991)). The landscape was initially overprinted by Antarctic Peninsula ice during the LGM. This ice sheet, and previous incarnations, has sculpted and moulded Ulu Peninsula. Variations in the thermal regime and ice stream activity have resulted in differences in the glacial drift. Following deglaciation, paraglacial and periglacial processes immediately began to modify the landscape (summarised in Fig. 13 and Table 2).

Our landsystem model (Fig. 13; Table 2) is a modern analogue to aid the interpretation of other high-latitude semi-arid environments during the Late Glacial in the Northern Hemisphere. Similar semi-arid environments are recognised to have existed during the Late Pleistocene in the Canadian High Arctic (Ó Cofaigh *et al.* 1999) and in Svalbard (Glasser & Hambrey 2003), and may be expected in high-latitude continental interiors glaciated during the LGM, such as Siberia and European Russia.

Glacial-paraglacial-periglacial interactions

A latitudinal transect from northern Chile through to the Dry Valleys highlights the changing dominance of different processes, driven primarily by the availability of meltwater (Fig. 14). It is clear that meltwater is increasingly important at more northerly latitudes. The fast-flowing temperate glaciers of the Northern Patagonian Icefield (47°S) produce large volumes of meltwater, which rapidly rework and remove fines generated subglacially. Subglacial landforms, such as drumlins, flutes, eskers, or crevasse-squeeze rides are rare (Glasser *et al.* 2009a). The large volume of meltwater results in numerous glaciofluvial ice-contact landforms, with abundant kame terraces, glacial lakes and raised lake shorelines, and rapid reworking of subglacially-deposited sediments and landforms. The meltwater also facilitates basal sliding and enables glaciers to flow quickly (Glasser *et al.* 2009a), resulting in abundant ice-scoured bedrock. In contrast, the sediment-landform assemblage around Tierra del Fuego, southernmost Chile (53°S), is dominated abundant subglacial till, flutes, drumlins and moraines, deposited by temperate glaciers but with reduced proglacial meltwater. Smaller sandur and ice-contact lakes, however, remain important (Benn & Clapperton 2000; Bentley *et al.* 2005). At these latitudes, there is only discontinuous permafrost at high altitudes (Trombotto 2002; Benn & Clapperton 2000), resulting in fewer rock glaciers, protalus ramparts, frost-shattered boulders or stone polygons than on James Ross Island. Aeolian processes are also comparatively less important; ventifacts and pebble-cobble lags are more numerous in East Antarctica than in Chile because of the comparatively faster, sand-bearing winds, less vegetation and less surficial sediments than in temperate regions.

On James Ross Island, freeze-thaw and fluvial activity have far greater relative importance when compared to the Dry Valleys (cf. French & Guglielmin 1999; Sugden *et al.* 1999; Hall & Denton 2005; McLeod *et al.* 2008), which significantly aids the development of patterned ground and solifluction landforms (Fig. 14). Indeed, the prevalence of moisture-driven periglacial processes on Ulu Peninsula contrasts sharply with their absence in more southerly, colder parts of Antarctica. In contrast, the Glacigenic Assemblage on James Ross Island resembles closely the cold-based glacial sediment-landform assemblages recognised in East Antarctica (Fig. 14; Atkins *et al.* 2002; Lloyd Davies *et al.* 2009; Hambrey & Fitzsimons 2010), perhaps indicating similarities between the climate during the LGM on James Ross Island and the climate in the Dry Valleys and East Antarctica today (cf. Fitzsimons 2003). Some paraglacial processes, such as glacio-isostatic adjustment, relaxation of rock walls, littoral reworking (González Bonorino *et al.* 1999) and fluvial reworking (albeit limited in the Dry Valleys) operate throughout the transect, although glacio-isostatic uplift, marine terraces and raised beaches are more prevalent at James Ross Island (cf. Roberts *et al.* 2011) and Tierra del Fuego, as a result of their proximity to the ocean.

The scope for landscape modification at the intersection of a paraglacial-periglacial-glacial landsystem is of great importance. Even in more temperate latitudes, the interplay between periglacial, paraglacial and glacial processes has been recognised as important (Coleman & Carr 2008). Ground ice is prevalent on James Ross Island today, in the form of permafrost, rock-glaciers, buried glacier ice and ice-cored moraines. Buried glacier ice can survive almost indefinitely in the permafrost environment (e.g., 8 m. yr. old ice in the Dry Valleys; Sugden *et al.* 1995; Schafer *et al.* 2000). However, despite the wealth of research on glacial and periglacial processes, there are relatively few papers that discuss the actions of one set of processes upon the other (Harris & Murton 2005).

The presence of permafrost beneath cold-based glaciers on James Ross Island during the LGM may have facilitated forward movement, as high porewater pressures beneath subglacial permafrost can reduce the shear strength of unfrozen substrate. This may also be a factor in initiating the large-scale mass movements. Further, proglacial permafrost can reduce effective stress by generating over pressuring in groundwater (Mathews & Mackay 1960; Boulton *et al.* 1995). Entrainment of debris (as observed in debris-rich basal ice exposed in ice-cored moraines) occurs through the transmission of basal shear stress from the glacier bed into the frozen subglacial sediment (Waller *et al*. 2009). The glacier couples with the permafrost (e.g. Cuffey *et al.* 2000), and the plane of movement (décollment plane) moves downwards to a plane of weakness within the underlying substrate, itself composed of relatively soft, easily deformable Cretaceous sediments. In this instance (cold-based glaciers overlying frozen ground), the base of the glacier is a heterogeneous zone, with the lower boundary of glacier flow varying spatially and temporally (Fitzsimons 2006; Waller *et al.* 2009).

This landsystem model includes many ice-cored landforms, such as ice-cored moraines, debris-covered glacier snouts, glacier-derived rock glaciers and talus-derived rock glaciers. The continuum and classification of ice-cored landforms has generated much debate (e.g., Hamilton & Whalley 1995; Humlum 1998; Konrad *et al.* 1999; Humlum 2000; Serrano & López-Martínez 2000; Lønne & Lyså 2005; Lukas *et al.* 2007; Degenhardt Jr 2009; Jacobs *et al.* 2011). The morphologies of landforms generated at the termini of polythermal and cold-based glaciers overlap significantly. For example, the processes governing the genesis of ice-cored moraine, debris-covered glacier termini, dead-ice moraine and glacier-derived rock glaciers may be very similar. However, these morphological terms describe different end members of the continuum, and their different processes, sediments and landforms are summarised in Table 6.

In the contemporary permafrost environment on James Ross Island, the seasonal melting of glacier ice and snow dominates sedimentary processes and products. However, this is modulated and modified by the melting and mobilisation of the permafrost active layer. In the semi-arid polar environment on James Ross Island, with predominantly cold-based glacial processes, periglaciation and paraglaciation dominating sediment transport. Sediment transfers occur through fluvial erosion, rock glaciers, slope instability and solifluction (cf. Harris & Murton 2005), and result in chaotic dead-ice terrain with abundant re-sedimentation processes (Etzelmüller & Hagen 2005). When analysing geomorphological processes in cold environments, glacial, periglacial and paraglacial processes must be considered as an intrinsically coupled system.

Character and behaviour of the LGM ice sheet on Ulu Peninsula

The basal thermal regime of ice sheets represents important empirical data required for numerical ice sheet models (Kleman *et al.* 1999; Siegert & Dowdeswell 2004; Siegert 2009). This research suggests that the subglacial thermal regime on Ulu Peninsula comprised four principal types: a wet-based ice stream, warm-based sheet flow, cold-based sheet flow and cold-based plateau ice caps. Each leaves a distinctive sediment-landform assemblage behind in the geological record (Table 7). The frozen-bed patches identified by Kleman and Glasser (2007) are more complex and variable than previously assumed. The thermal regime of Whisky Glacier and glaciers in Croft Bay is unknown. It is possible, however, that slippery marine sediments in the bays would have encouraged rapid basal sliding. Marine geological evidence has been taken to suggest that cold-based ice developed on the Antarctic Peninsula mountains (Ó Cofaigh *et al.* 2001; Reinardy *et al.* 2009). Unglacierised mesas are assumed to have been above the height of the LGM ice sheet, but they could have harboured cold-based plateau ice caps (Johnson *et al*. 2009). If the mesas were above the LGM ice sheet, the summit plateau elevations provide an estimate for maximum ice thicknesses at the LGM. However, an ice surface elevation of c. 750 m a.s.l. has been demonstrated for Dobson Dome, just south of our field area (Fig. 1), with an age of < 80 ka (with large errors; Smellie *et al.* 2008).

Sharp boundaries in thermal regime and styles of erosion and deposition have long been recognised in the geological record at the shear margins of ice streams (Stokes & Clark 1999, 2001). Less is known about flow boundary patterns in sheet-flow areas. However, on Ulu Peninsula, the mosaic in the thermal regime of the cold-based ice sheet operating under sheet-flow was subtle, and the boundaries more dispersed than the shear margins of ice streams.

The glacial sandy boulder gravel that characterises James Ross Island today is a significant contrast to the Neogene diamictite logged in many locations across the island (Hambrey & Smellie 2006; Hambrey *et al.* 2008; Smellie *et al.* 2009). Similar contrasts have been noted in the Dry Valleys, where pebble gravels deposited by cold-based ice differ from Neogene the Sirius Group diamictons (Hambrey & Fitzsimons 2010). This is indicative of changing climatic regimes, with diamicton, silt and clay forming only under the warmer climatic conditions of the Neogene (cf. DeConto & Pollard 2003; Mayewski *et al.* 2009). Warmer atmospheric temperatures encouraged subglacial sliding, erosion, transportation and deposition under a wet-based ice sheet, with abundant production of fines and therefore diamictites. Abrasion under cold-based glaciers is insufficient to generate the large quantities of fines required for subglacial till formation, which is associated with warm-based glaciers above the pressure melting point. Geothermal heating may also have aided the production of basal meltwater and subglacial till formation during the Neogene Period on James Ross Island (Hambrey *et al.* 2008). Effects of volcanically enhanced geothermal gradients on meltwater availability during the Neogene are difficult to determine. However, those effects were probably localised mainly to within several km of the erupting vents (at Mount Haddington, c. 40 km distant), with only a very limited influence likely in the more distal regions where our study was focussed. Quaternary volcanic activity was somewhat closer, situated on western Vega Island, Terrapin Hill and Dobson Dome (990 ka, c. 660 ka and < 80 ka, respectively, the latter two with large errors; Smellie *et al.* 2008), situated c. 10, 20 and 10 km, respectively, from our field area. The Quaternary centres are therefore probably too old and too distant to have had a major effect in the Brandy Bay area.

This study has shown that cold-based ice sheets are capable of entraining and moving sub-glacial sediments and boulders, and, in conjunction with numerous recent studies that illustrate the erosive and depositional capabilities of ice sheets that reach -17°C at their bed (e.g., Phillips *et al.* 2006; Hambrey & Fitzsimons 2010), supports a new and emerging paradigm of sheet flow in high latitude regions. The old paradigm suggested that ice sheets comprised a patchwork of cold-based ice on mountain tops, with very little erosion or deposition, surrounded by highly active warm-based ice that typically occupied valleys (e.g., Hättestrand & Stroeven 2002; Stroeven *et al.* 2002; Briner *et al.* 2003; Davis *et al.* 2006). Delicate structures and blockfields are preserved at high altitudes (Kleman *et al.* 1999; Johnson *et al.* 2009). New and emerging research (for examples, see Kleman & Glasser 2007) suggests that this is an over-simplification, and that sheet flow beneath high-latitude ice sheets is more complex. Although cold-based glaciers are weak erosional and depositional agents compared with warm-based glaciers, the interaction between glaciers, their thermal regime and their beds is more subtle than is usually assumed (Cuffey *et al.* 2000; Lloyd Davies *et al.* 2009). The ice sheet that overwhelmed James Ross Island during the LGM was a composite of ice streaming in the trough of Prince Gustav Channel, which impinged on the coastal margins of Ulu Peninsula; sheet flow on the main part of Ulu Peninsula with both warm and cold-based ice flowing across the island, and cold-based and stationary plateau ice domes on high plateau blockfields (Table 7). The lateral margins of Prince Gustav Ice Stream were likely to have been dominated by warm-based sheet flow; the evidence for this includes moraines and enhanced deposition of erratics. The key point of this new paradigm is that the cold-based ice was capable of movement, erosion, transportation of material and deposition, with enhanced deposition occurring in small areas as a result of changes in the thermal regime of the ice sheet, and that sheet flow and cold-based ice are more complex than previously thought.

Conclusions

This holistic and systematic study of sediment-landform assemblages from Ulu Peninsula on James Ross Island (Table 2) has used detailed sedimentary descriptions, clast lithology, shape-roundness counts and geomorphology mapped both in the field and from remotely-sensed images (Table 1) to discriminate six sediment-landform assemblages and thus to present the first landsystem model from a semi-arid sub-polar desert from the Antarctic Peninsula. The conceptual model in Fig. 13 emphasises the interrelationship and importance of not only glacial, but also periglacial and paraglacial processes. The six sediment-landform assemblages identified were, 1) the Glacier Snow and Ice Assemblage; 2) the Glacigenic Assemblage; 3) the Boulder Train Assemblage, 4) the Ice-Cored Moraine Assemblage; 5) the Paraglacial Assemblage and 6) the Periglacial Assemblage. Analysis if these assemblages provides a detailed understanding of landscape evolution on James Ross Island. Sediments and landforms were deposited during LGM glaciation and from mid to late-Holocene glacier readvances. These were subsequently reworked and redeposited by periglacial and paraglacial processes throughout the Holocene and into the present day. Crucially, when compared with the few other polar landsystem models, we find that the availability of melt water encourages strong landform modification by periglacial processes. These processes would have been similarly important in the Northern Hemisphere during the Late Pleistocene epoch. Therefore the landsystem model presented here is a modern analogue to be used in the interpretation of past glaciated environments.

This paper presented new information regarding the thermal regime of the Antarctic Peninsula Ice Sheet during LGM glaciation (Table 7). The data and model for the interplay between cold-based, warm-based and streaming ice challenges the theory that cold-based glaciers do not erode or deposit. We have presented geomorphological and sedimentological data to help interpret the presence of cold-based sheet flow in other Quaternary glaciated environments. Finally, this paper presented important new data regarding the thermal regime and character and behaviour of the LGM ice sheet on James Ross Island, which will aid reconstructions of the LGM ice sheet in northern Antarctic Peninsula.

The authors gratefully acknowledge funding from the Natural Environment Research Council (NERC) grant through the Antarctic Funding Initiative (grant AFI 9-01; NE/F012942/1). Fieldwork was logistically supported by the British Antarctic Survey, and the authors thank Alan Hill for assistance in the field and the captains and crew of the *RRV Ernest Shackleton* and the *RRV James Clark Ross* for their cooperation and support. Daniel Nývlt's field research and digital data preparation was funded from the R & D project VaV SP II 1a9/23/07, financed by the Ministry of the Environments of the Czech Republic. We thank the crew of Mendel Station for logistic support in the field. The authors acknowledge Etienne Berthier and the Centre National d'Etudes Spatiales (CNES) for the SPOT-5 images. The Czech Geological Survey are thanked for providing the orthophoto mosaic from 2006 aerial photographs, DEM and GIS vector files from their map of Ulu Peninsula, published in 2009. The Antarctic Digital Database is acknowledged for providing formal glacier names.

Tables

Table 1. Sources used for remote mapping of landforms. RMS = Root Mean Square error.

Data Source	Resolution / Scale	Date Captured	Notes
BAS/JR/2/79	1:95 000	February 1979	BAS and Royal Navy aerial photographs taken over Brandy Bay, Vega Island, Rum Cove and Terrapin Hill. Digitally scanned and georeferenced in ArcGIS to SPOT-5 satellite images (WGS84 UTM 21 S). Photographs copyright British Antarctic Survey and Crown copyright Controller of Her Majestey's Stationary Office and the UK Hydrographic Office. The 2006 aerial photographs were processed, georeferenced and orthorectified by Nývlt and Šerák (Czech Geological Survey, 2009).
BAS/JR/1/79	1:95 000	January 1979	
BAS/JR/2/80	1:95 000	February 1980	
RN/6/89	1:16 000	January 1989	
BAS/RN/06	1:25 000 (< 1 m)	2006 (various dates)	
Digital Elevation Model (DEM) produced by Nývlt and Šerák (Czech Geological Survey 2009)	< 5 m	Created from BAS 1970/80 and 2006 aerial photographs	James Ross Island – Northern Part. Heights: geoid EGM96. Map projection: WGS84 UTM 21S

Table 2. Summary of the six sediment-landform assemblages on Ulu Peninsula, James Ross Island

Assemblage	Principle land elements	Age of formation	Interpretation
Glacier snow and ice assemblage	Glacier ice (cirque, tidewater, valley, dome glaciers) Perennial snow-banks	Holocene to present day	Contemporary glaciation. Small cold-based cirque and plateau glaciers dominate on Ulu Peninsula.
Glacigenic assemblage	Erratic-poor drift Cretaceous bedrock with scattered basalts Erratic-rich drift (in coastal regions) Erratic-rich drift (in cols and passes) Moraine fragments	LGM	James Ross Island overwhelmed by the Antarctic Peninsula Ice Sheet. Development of Prince Gustav Ice Stream in Prince Gustav Channel.
Boulder train assemblage	Boulder train Erratic-poor drift sheet "Brandy Bay Moraine" (with some reworked granite erratics) "IJR-45 Glacier Moraine"	Mid-Holocene	Mid-Holocene readvance of "IJR-45" to form a marine-terminating glacier in Brandy Bay.
Ice-cored moraine assemblage	Ice-cored moraines in front of cirques (both with and without modern glaciers)	Late-Holocene	Late-Holocene readvance of small polythermal glaciers, possibly during a southern Hemisphere equivalent of the "Little Ice Age".
Paraglacial assemblage	Scree slopes Boulder lags on beaches Ventifacts ; cobble-boulder pavements Spits and beaches Marine terraces Rivers and streams	Holocene to present day	Paraglacial reworking of glacigenic sediments and landforms
	Large scale mass movements	Neogene to present	Paraglacial relaxation of basalt deltas
Periglacial assemblage	Rock glaciers Nivation hollows Protalus and pronival ramparts Freeze-thaw shattering of boulders Solifluction	Holocene to present day	Periglaciation of James Ross Island, with deep permafrost and a seasonal active layer.
	Mesas and blockfields	(Neogene to present day)	Development of blockfields shortly after their genesis in the Neogene. Occasionally glaciated by small, cold-based plateau glaciers.

Table 3. Principal characteristics of the land-terminating glaciers on Ulu Peninsula (after Davies *et al.* submitted). San José and Lachman glaciers are treated as one glacier. "Width" was measured at the widest point on the glacier. ELA is calculated from topographical data (refer to Davies *et al*. submitted for more information). Refer to Fig. 2 for glacier locations.

Glacier	Type	Length	Width	Area	Mean Slope	ELA (m a.s.l.)	Recession rate 1988 to 2009
"IJR-45"*	Valley glacier	3.26 km	0.8 km	2.36 km^2	5°	270 m	0.144 $km^2\ a^{-1}$
"Unnamed Glacier"	Cirque glacier	2.53 km	0.5 km	3.61 km^2	12°	350 m	0.017 $km^2\ a^{-1}$
Triangular Glacier	Cirque glacier	0.9 km	0.8 km	0.62 km^2	17°	180 m	0.004 $km^2\ a^{-1}$
Lachman and San José Glaciers	Cirque glacier	1.44 km	1.5 km	0.62 km^2	12°	230 m	0.000 $km^2\ a^{-1}$
Alpha Glacier	Valley glacier	3.94 km	1.0 km	3.19 km^2	8°	230 m	0.016 $km^2\ a^{-1}$
Davies Dome	Dome (plateau) glacier	3.46 km	2.7 km	6.46 km^2	9 °	300 m	0.041 $km^2\ a^{-1}$

*Informally named "Whisky Glacier" by Chinn & Dillon (1987); name not used here as it clashes with officially adopted name for the glacier (Whisky Glacier) between Dobson Dome and Whisky Bay (British Antarctic Survey 2010). "IJR-45" from Rabassa *et al.* 1982.

Table 4. Glacigenic Assemblages: LGM sediments and landforms of James Ross Island. TPG: Trinity Peninsula Group metamorphic rocks (cf. Fig. 1).

Land element	Sediments	Landforms	Processes and interpretation	Age
Erratic-poor drift; basalt pebble-cobble gravel	Subangular to subrounded clasts, numerous basalt and rare granite boulders either well-embedded in sediments or perched on surface. Pebble lags, ventifacts and desert varnish are common.	Smooth, flat surfaces. Widespread across the interior of Ulu Peninsula.	Deposition beneath a slow-moving cold-based ice sheet	LGM
Erratic-poor drift; sandstone and siltstone breccia	Unlithified sandstone / siltstone regolith, poorly-compacted, occasional isolated granite or basalt boulders; scattered basalt cobbles across the surface	Smoothed surfaces, occasionally bedding planes are visible.	Scouring and deposition beneath a cold-based ice sheet	LGM
Erratic-rich coastal 'drift sheet' with abundant TPG & granite erratics	Found along the western coast of Ulu Peninsula. Subangular to subrounded clasts, numerous boulders and pebbles of Trinity Peninsula origin.	Constructional ridges, moraine fragments, smooth slopes. Focussed in coastal areas and where ice flow is concentrated.	Deposition beneath fast-flowing, warm-based ice, adjacent to Prince Gustav Ice Stream. Lateral moraines were formed by Prince Gustav Ice Stream.	LGM
Erratic-rich patchy 'drift sheet' with TPG & granite erratics	Found in cols and passes. Subangular to subrounded clasts, numerous boulders and pebbles of Trinity Peninsula origin.	Occasional moraine fragments; streamlined bedrock (hyaloclastite) ridges; smoothed cols and passes.	Deposition beneath wet-based ice; sheet flow. Moraines and streamlined features were formed by inland wet-based sheet flow	LGM

Table 5. Description and characteristics of the principle zones associated with the large moraine in front of "IJR-45".

Zone	Sediments	Landforms	Interpretation
Zone 1	Thin drape of fine pebble-gravel at the margin. Largely clean glacier ice	Stratified white and blue ice, supraglacial streams.	Glacier ice; minor debris cover
Zone 2	Surface varies from silt-rich diamicton to angular sandy boulder gravel, angular to striated boulders and cobbles. Occasional striated boulders.	Series of small, thin, sharp-crested ridges, numerous small lakes (< 10 m diameter), scars with exposed stratified ice (sediment drape is 20-40 cm thick), conical mounds of sediment, large boulders resting on pedestals of ice. Complex and chaotic topography. Lines of boulders on ridges. Small debris flows.	Fresh ice-cored moraine
Zone 3	Sandy boulder gravel surface with matrix composed of weathered hyaloclastite. Occasional fines in association with numerous sandstone boulders.	Moraine widens and flattens. 5 m high sharp-crested to more subtle ridges. Isolated mounds. Ice collapse pits. Occasional small ice scars and buried ice under ridges. Lines of hyaloclastite boulders on ridges. Perched boulders. Crescent-shaped scars. Perched lakes. Ridges increasingly subdued with distance from the ice margin.	Degrading ice-cored moraine
Zone 4	Lag of pebbles and boulders on surface. Sandy boulder-gravel. Frost-shattered basalt.	Subsiding and subdued ridge crests, debris flows, perched and frozen lakes, no visible ice, sandy boulder gravel surface. Basalt and hyaloclastite boulders wasting down *in situ*. Incipient stone stripes and polygon nets.	Dead-ice moraine
Zone 5	Fines are absent from the surface, leaving a cobble-pebble lag. Basalt and weathered hyaloclastite boulders. Well-developed stone stripes and polygon nets. Frost-shattered basalt.	Low-relief and subtle ridge crests, no visible ice, sandy boulder gravel surface. Small incised and snow-patch fed streams. Steep frontal edge off moraine. Solifluction lobes move downslope on steep frontal face and where streams have incised. Evidence of former ice-core, including debris flows, subsiding ridge crests, weathering hyaloclastite boulders. Drained lakes leaving depressions.	Dead-ice moraine; Permafrost

Table 6. Continuum of ice-cored features in a glacial-periglacial landscape, and criteria for recognition in the landform record.

Landform	Criteria for identification	Processes of formation	References and examples	Geomorphological significance
Debris covered glacier	Uniformly thin debris layer on glacier surface.	Thrusting and upwards movement of ice transport subglacial debris to surface. Meltout of englacial debris bands. Ridges mimic the surface of the glacier. Thin debris cover.	Lukas *et al.* 2007; Jacobs *et al.* 2011	Stagnation of glacier snout; melting and down-wasting *in situ.*
Ice-cored moraine	• Thrusts • Exposed stratified and debris-rich ice • Perched ponds and boulders • Debris flows and slumps • Possibly striated clasts / boulders.	Thrusts are caused by compressive stresses at frozen glacier margins in small polythermal glaciers. Debris entrained in basal ice is thrust towards the surface. Melting and back wasting of ice results in release of debris to the surface, where it is redistributed and resedimented by meltwater, debris flows and slumps. Debris may be supplemented by supraglacial material.	Østrem 1964; 1971; Hambrey *et al.* 1999; Glasser & Hambrey 2003; Schomacker & Kjær 2007; Schomacker 2008	Polythermal glacial conditions. Crest denotes the maximum extent of the glacier.
Dead-ice moraine	• Hummocky landscape • Subdued ridges • Perched boulders • No visible ice scars.	Down-wasting and back-wasting of ice scars and increased burial by talus. Top and bottom melt. Lowering of moraine surface. Extensive sediment redistribution. Further ice melting is limited by the insulating effect of the debris mantle. Thick debris cover. Ice stagnation and little active melting.	Kjær & Krüger 2001; Schomacker & Kjær 2007, 2008; Krüger *et al.* 2010; Klint *et al.* 2011	Periglacial environment. May indicate the extent of a former advance.
Glacier-derived rock glacier	• Core of glacial ice (with stratification) • Down-slope movement • Lobate shape. Furrows, ridges and mounds on surface • Continuous, thick debris cover • Very small accumulation area • Steep frontal and side slopes	Downslope movement of ice/debris mixtures by creep. Talus falls onto glacier surface, resulting in a thick debris cover, accumulating on low-angle slopes. This insulates the ice and limits ablation. Surface debris rolling down the stoss side is overridden, forming a sub-rock glacier debris layer. Strongly developed surface relief can indicate compressive stress.	Hamilton & Whalley 1995; Konrad *et al.* 1999	May indicate location of palaeo-ice margin. Periglacial conditions. Forms a continuum with ice-cored moraine. Indicative of limited precipitation.
Talus-derived rock glacier (also known as protalus lobes)	• Downslope movement • Large talus supply (e.g. scree) • Form below cliffs or steep terrain • Distinct ridge and furrow pattern • Steep front and side slopes • Ponds and glacial karst landscape	Accumulation of ice and debris in the upper part of the rock glacier. The ice-rock mixture flows downslope, with ice ablating slowly at the base of the active layer.	Hamilton & Whalley 1995; Serrano & López-Martínez 2000; Degenhardt Jr 2009	Periglacial; frequent freeze-thaw cycles, sub-zero ground temperatures, abundant talus supply, limited precipitation.

Table 7. Principal land elements of the Glacigenic Assemblage and inferred subglacial thermal regime.

Glacial Drift	Characteristics	Inferred thermal regime
Erratic-poor glacial drift	Sandy boulder gravel found widely across the island; smooth slopes. Basalt and Cretaceous lithologies only.	Cold-based sheet flow
Erratic-poor glacial drift	On mesas and around Davies Dome. Smooth and flat; no landforms.	Cold-based plateau ice cap
Erratic-rich drift (in cols and passes)	Sandy boulder gravel at higher elevations in cols and passes. Up to 30 % Trinity Peninsula erratics. Smoothed and sculpted cols.	Warm-based sheet flow
Erratic-rich drift (in coastal regions)	Sandy boulder gravel with up to 50 % erratics from Trinity Peninsula. Associated with moraine fragments.	Ice stream

5 References

ADAM, W.G. & KNIGHT, P.G. 2003. Identification of basal layer debris in ice-marginal moraines, Russell Glacier, West Greenland. *Quaternary Science Reviews*, **22**, 1407-1414.

ATKINS, C.B., BARRETT, P.J. & HICOCK, S.R. 2002. Cold glaciers erode and deposit: evidence from Allan Hills, Antarctica. *Geology*, **30**, 659-662.

AUGUSTINUS, P.C. 2002. Weathering characteristics of the glacial drifts, Bunger Hills, East Antarctica. *Arctic, Antarctic, and Alpine Research*, **34**, 65-75.

BALLANTYNE, C.K. 1991. Scottish landform examples 2 - the landslides of Trotternish, Isle of Skye. *Scottish Geographical Magazine,* **107**, 130-135.

BALLANTYNE, C.K., STONE, J.O. & FIFIELD, L.K. 1998. Cosmogenic Cl-36 dating of postglacial landsliding at The Storr, Isle of Skye, Scotland. *The Holocene,* **8**, 347-351.

BALLANTYNE, C.K. 2002. Paraglacial geomorphology. *Quaternary Science Reviews*, **21**, 1935-2017.

BALLANTYNE, C.K. 2007. Periglacial Landforms: Patterned Ground. In Scott, A.E. (ed) *Encyclopedia of Quaternary Science,* Oxford: Elsevier, 2182-2191.

BALLANTYNE, C.K. 2010. A general model of autochthonous blockfield evolution. *Permafrost and Periglacial Processes*, **21**, 289-300.

BARBEAU, D.L., DAVIS, J.T., MURRAY, K.E., VALENCIA, V., GEHRELS, G.E., ZAHID, K.M. & GONBOSI, D.J. 2010. Detrital-zircon geochronology of the metasedimentary rocks of north-western Graham Land. *Antarctic Science*, **22**, 65-78.

BENN, D.I. & CLAPPERTON, C.M., 2000. Pleistocene glaciotectonic landforms and sediments around central Magellan Strait, southernmost Chile: evidence for fast outlet glaciers with cold-based margins. *Quaternary Science Reviews,* **19**, 591-612.

BENN, D.I. & BALLANTYNE, C.K. 1994. Reconstructing the transport history of glacigenic sediments: a new approach based on the co-variance of clast form indices. *Sedimentary Geology*, **91**, 215-227.

BENN, D.I. & LUKAS, S. 2006. Younger Dryas glacial landsystems in North West Scotland: an assessment of modern analogues and palaeoclimatic implications. *Quaternary Science Reviews*, **25**, 2390-2408.

BENN, D.I. & EVANS, D.J.A., 2010. *Glaciers & Glaciation*. Hodder Education, London, 802 pp.

BENNETT, M.R., HUDDART, D., GLASSER, N.F. & HAMBREY, M.J. 2000a. Resedimentation of debris on an ice-cored lateral moraine in the high-Arctic (Kongsvegen, Svalbard). *Geomorphology*, **35**, 21-40.

BENNETT, M.R., HUDDART, D. & WALLER, R.I. 2000b. Glaciofluvial crevasse and conduit fills as indicators of supraglacial dewatering during a surge, Skeiðarárjökull, Iceland. *Journal of Glaciology*, **46**, 25-34.

BENTLEY, M.J., SUGDEN, D.E., HURLTON, N.R.J. & MCCULLOCH, 2005. The landforms and pattern of deglaciation in the Strait of Magellan and Bahía Inútil, southernmost America. *Geografiska Annaler,* **87A**, 313-333.

BERTLER, N.A.N., MAYEWSKI, P.A. & CARTER, L. 2011. Cold conditions in Antarctica during the Little Ice Age - implications for abrupt climate change mechanisms. *Earth and Planetary Science Letters*, **308**, 41-51.

BIBBY, J.S. 1966. *The stratigraphy of part of north-east Graham Land and the James Ross Island Group*. British Antarctic Survey, London, 37 pp.

BJÖRCK, S., OLSSON, S., ELLIS-EVANS, C., HÅKANSSON, H., HUMLUM, O. & DE LIRIO, J.M. 1996. Late Holocene palaeoclimatic records from lake sediments on James Ross Island, Antarctica. *Palaeogeography, Palaeoclimatology, Palaeoecology*, **121**, 195-220.

BOCKHEIM, J.G. 2010. Evolution of desert pavements and the vesicular layer in soils of the Transantarctic Mountains. *Geomorphology*, **118**, 433-443.

GONZÁLEZ BONORINO, G., BUJALESKY, G., COLOMBO, F. & FERRERO, M. 1999. Holocene coastal palaeoenvironments in Atlantic Patagonia, Argentina. *Journal of South American Earth Sciences,* **12**, 325-331.

BOULTON, G.S. 1972. Modern Arctic glaciers as depositional models for former ice sheets. *Journal of the Geological Society of London*, **128**, 361-393.

BOULTON, G.S., CABAN, P.E., & VAN GIJSSEL, K. 1995. Groundwater flow beneath ice sheets: Part II – its impact on glacier tectonic structures and moraine formation. *Quaternary Science Reviews*, **14**, 563-587.

BOULTON, G.S. & DENT, D.L. 1974. The nature and rate of post-depositional changes in recently deposited till from south-east Iceland. *Geografiska Annaler*, **56A**, 121-134.

BRIDGLAND, D.R. 1986. *Clast Lithological Analysis. Technical Guide No. 3.* Quaternary Research Association, Cambridge, 207 pp.

BRINER, J.P., MILLER, G.H., DAVIS, P.T., BIERMAN, P.R. & CAFFEE, M. 2003. Last Glacial Maximum ice sheet dynamics in Arctic Canada inferred from young erratics perched on ancient tors. *Quaternary Science Reviews*, **22**, 437-444.

BRITISH ANTARCTIC SURVEY 2010. Antarctic Sound and James Ross Island, Northern Antarctic Peninsula. *Series BAS (UKAHT) Sheets 3A and 3B, 1:250000,* Cambridge.

CAMERLENGHI, A., DOMACK, E., REBESCO, M., GILBERT, R., ISHMAN, S., LEVENTER, A., BRACHFELD, S. & DRAKE, A. 2001. Glacial morphology and post-glacial contourites in northern Prince Gustav Channel (NW Weddell Sea, Antarctica). *Marine Geophysical Researches*, **22**, 417-443.

CARRIVICK, J.L., DAVIES, B.J., GLASSER, N.F. & NÝVLT, D. submitted. Late Holocene changes in character and behaviour of land-terminating glaciers on James Ross Island, Antarctica. *Journal of Glaciology*.

CHINN, T.J.H. & DILLON, A. 1987. Observations on a debris-covered polar glacier "Whisky Glacier", James Ross Island, Antarctic Peninsula, Antarctica. *Journal of Glaciology*, **33**, 300-310.

CLAYTON, L. 1964. Karst topography on stagnant glaciers. *Journal of Glaciology*, **5**, 107-112.

COLEMAN, C.G. & CARR, S.J. 2008. Complex relationships between Younger Dryas glacial, periglacial and paraglacial landforms, Brecon Beacons, South Wales. *Proceedings of the Geologists' Association*, **119**, 259-276.

CUFFEY, K.M., CONWAY, H., GADES, A.M., HALLET, B., LORRAIN, R., SEVERINGHAUS, J.P., STEIG, E.J., VAUGHN, B. & WHITE, J.W.C. 2000. Entrainment at cold glacier beds. *Geology*, **28**, 351-354.

CUFFEY, K.M., CONWAY, H., HALLET, B., GADES, A.M. & RAYMOND, C.F. 1999. Interfacial water in polar glaciers and glacier sliding at -17°C. *Geophysical Research Letters*, **26**, 751-754.

CZECH GEOLOGICAL SURVEY 2009. James Ross Island - Northern Part. Topographic Map 1:25 000. Praha: Czech Geological Survey.

DAVIES, B.J., HAMBREY, M.J., SMELLIE, J.L., CARRIVICK, J.L. & GLASSER, N.F. 2011. Antarctic Peninsula Ice Sheet evolution during the Cenozoic Era. *Quaternary Science Reviews* in press.

DAVIES, B. J., CARRIVICK, J. L., GLASSER, N. F., HAMBREY, M. J., & SMELLIE, J. L. submitted. A new glacier inventory for 2009 reveals spatial and temporal variability in glacier response to atmospheric warming in the northern Antarctic peninsula, 1988-2009. *The Cryosphere Discussions*.

DAVIS, P.T., BRINER, J.P., COULTHARD, R.D., FINKEL, R.W. & MILLER, G.H. 2006. Preservation of Arctic landscapes overridden by cold-based ice sheets. *Quaternary Research*, **65**, 156-163.

DECONTO, R.M. & POLLARD, D. 2003. Rapid Cenozoic glaciation of Antarctica induced by declining atmospheric CO_2. *Nature*, **421**, 245-249.

DEGENHARDT JR, J.J. 2009. Development of tongue-shaped and multilobate rock glaciers in alpine environments - interpretations from ground penetrating radar surveys. *Geomorphology*, **109**, 94-107.

DOMACK, E.W., BURNETT, A. & LEVENTER, A. 2003. Environmental setting of the Antarctic Peninsula. *In* DOMACK, E., LEVENTER, A., BURNETT, A., BINDSHADLER, R., CONVEY, P. & KIRBY, M. (eds) *Antarctic Peninsula Climate Variability: Historical and Paleoenvironmental Perspectives*, Antarctic Research Series, **79**, American Geophysical Union, Washington, 1-13.

ENGEL, Z., NÝVLT, D. & LÁSKA, K. submitted. Ice thickness, bed topography and glacier volume changes on James Ross Island, Antarctic Peninsula. *Journal of Glaciology*.

ENGEL, Z., LÁSKA, K., FRANTA, T., MÁČKA, Z. & MARVÁNEK, O. 2010. Recent Changes of Permafrost Active Layer on the James Ross Island, Maritime Antarctic. *In* Abstracts from the Third European Conference on Permafrost, 13-1ý June 2010, Svalbard, p. 129.

ERMOLIN, E., DE ANGELIS, H. & SKVARCA, P. 2002. Mapping of permafrost on Vega Island, Antarctic Peninsula, using satellite images and aerial photography. *Annals of Glaciology*, **34**, 184-188.

ERMOLIN, E., DE ANGELIS, H., SKVARCA, P. & RAU, F. 2004. Ground ice in permafrost on Seymour (Marambio) and Vega Islands, Antarctic Peninsula. *Annals of Glaciology*, **39**, 373-378.

ETZELMÜLLER, B. & HAGEN, J.O. 2005. Glacier-permafrost interaction in Arctic and alpine mountain environments with examples from Norway and Svalbard. In: HARRIS, C. & MURTON, J.B. 2005. *Cryospheric systems: glaciers and permafrost.* Geological Society, London, Special Publications, **242**, 11-27.

EVANS, D.J.A. 1993. High-latitude rock glaciers: A case study of forms and processes in the Canadian arctic. *Permafrost and Periglacial Processes*, **4**, 17-35.

EVANS, D.J.A. 2003a. Ice-marginal terrestrial landsystems: active temperate glacier margins. *In* EVANS, D.J.A. (ed) *Glacial Landsystems,* Arnold, London, 12-43.

EVANS, D.J.A. 2003b. Introduction to glacial landsystems. *In* EVANS, D.J.A. (ed) *Glacial Landsystems,* Arnold, London, 1-11.

EVANS, D.J.A. 2009. Controlled moraines: origins, characteristics and palaeoglaciological implications. *Quaternary Science Reviews*, **28**, 183-208.

EVANS, D.J.A. 2011. Glacial landsystems of Satujökull, Iceland: A modern analogue for glacial landsystem overprinting by mountain icecaps. *Geomorphology*, **129**, 225-237.

EVANS, D.J.A. & TWIGG, D.R. 2002. The active temperate glacial landsystem: a model based on Breiethamerkurjokull and Fjallsjokull, Iceland. *Quaternary Science Reviews*, **21**, 2143-2177.

EVANS, D.J.A. & BENN, D.I. 2004. Facies description and the logging of sedimentary exposures. *In* EVANS, D.J.A. & BENN, D.I. (eds) *A practical guide to the study of glacial sediments,* Arnold, London, 11-50.

EVANS, D.J.A., PHILLIPS, E.R., HIEMSTRA, J.F. & AUTON, C.A., 2006. Subglacial till: Formation, sedimentary characteristics and classification. *Earth-Science Reviews,* **78**, 115-176.

EVANS, J., PUDSEY, C.J., Ó COFAIGH, C., MORRIS, P. & DOMACK, E. 2005. Late Quaternary glacial history, flow dynamics and sedimentation along the eastern margin of the Antarctic Peninsula Ice Sheet. *Quaternary Science Reviews*, **24**, 741-774.

FITZSIMONS, S.J. 1996. Paraglacial redistribution of glacial sediments in the Vestfold Hills, East Antarctica. *Geomorphology*, **15**, 93-108.

FITZSIMONS, S.J. 2003. Ice-marginal terrestrial landsystems: polar continental glacier margins. *In* EVANS, D.J.A. (ed) *Glacier Landsystems,* Hodder, London, 89-110.

FITZSIMONS, S. 2006. Mechanical behaviour and structure of the debris-rich basal ice layer. *In:* KNIGHT, P.G. (ed.) *Glacier Science & Environmental Change.* Blackwell, Oxford, 329-335.

FITZSIMONS, S.J., MCMANUS, K.J. & LORRAIN, R.D. 1999. Structure and strength of basal ice and substrate of a dry-based glacier: evidence for substrate deformation at sub-freezing temperatures. *Annals of Glaciology*, **28**, 236-240.

FITZSIMONS, S., WEBB, N., MAGER, S., MACDONELL, S., LORRAIN, R. & SAMYN, D. 2008. Mechanisms of basal ice formation in polar glaciers: An evaluation of the apron entrainment model. *Journal of Geophysical Research*, **113**, F02010.

FRENCH, H.M. 1988. Active layer processes. *In* CLARK, M.J. (ed) *Advances in periglacial geomorphology,* Wiley-Interscience, Chichester,151-178.

FRENCH, H.M. & GUGLIELMIN, M. 1999. Observations on the ice-marginal, periglacial geomorphology of Terra Nova Bay, Northern Victoria Land, Antarctica. *Permafrost and Periglacial Processes*, **10**, 331-347.

FUKUDA, M., STRELIN, J.A., SHIMOKAWA, K., TAKAHASHI, N., SONE, T. & TROMBOTT, D. 1992. Permafrost occurrence of Seymour Island and James Ross Island, Antarctic Peninsula region. *In* YOSHIDA, N., KAMINUMA, K. & SHIRAISHI, K. (eds) *Recent progress in Antarctic Earth Sciences,* Terra Scientific Publishing Company (TERRAPUB), Tokyo, 745-750.

FUKUI, K., SONE, T., STRELIN, J.A., TORIELLI, C.A. & MORI, J. 2007. Ground penetrating radar sounding on an active rock glacier on James Ross Island, Antarctic Peninsula region. *Polish Polar Research*, **28**, 13-22.

FUKUI, K., SONE, T., STRELIN, J.A., TORIELLI, C.A., MORI, J. & FUJII, Y. 2008. Dynamics and GPR stratigraphy of a polar rock glacier on James

Ross Island, Antarctic Peninsula. *Journal of Glaciology*, **54**, 445-451.

GALE, S.J. & HOARE, P.G. 1991. *Quaternary Sediments: Petrographic methods for the study of unlithified rocks.* New York: John Wiley & Sons. 323 pp.

GILBERT, R., DOMACK, E.W. & CAMERLENGHI, A. 2003. Deglacial history of the Greenpeace trough: Ice sheet to ice shelf transition in the Northwestern Weddell Sea. *In* DOMACK, E., LEVENTER, A., BURNETT, A., BINDSHADLER, R., CONVEY, P. & KIRBY, M. (eds) *Antarctic Peninsula Climate Variability: Historical and Paleoenvironmental Perspectives,* Antarctic Research Series, **79**, American Geophysical Union, Washington, 195-204.

GLASSER, N.F. & HAMBREY, M.J. 2003. Ice-marginal terrestrial landsystems: Svalbard polythermal glaciers. *In* EVANS, D.J.A. (ed) *Glacier Landsystems,* Hodder, London, 65-87.

GLASSER, N.F. & JANSSON, K.N. 2005. Fast-flowing outlet glaciers of the Last Glacial Maximum Patagonian Icefield. *Quaternary Research*, **63**, 206-211.

GLASSER, N.F., HAMBREY, M.J., CRAWFORD, K.R., BENNETT, M.R. & HUDDART, D. 1998. The structural glaciology of Kongsvegen, Svalbard, and its role in landform genesis. *Journal of Glaciology*, **44**, 136-148.

GLASSER, N.F., JANSSON, K.N., HARRISON, S. & RIVERA, A. 2005. Geomorphological evidence for variations of the North Patagonian Icefield during the Holocene. *Geomorphology*, **71**, 263-277.

GLASSER, N.F., HARRISON, S. & JANSSON, K.N. 2009a. Topographic controls on glacier sediment-landform associations around the temperate North Patagonian Icefield. *Quaternary Science Reviews*, **28**, 2817-2832.

GLASSER, N.F., KULESSA, B., LUCKMAN, A., JANSEN, D., KING, E.C., SAMMONDS, P.R., SCAMBOS, T.A. & JEZEK, K.C. 2009b. Surface structure and stability of the Larsen C Ice Shelf, Antarctic Peninsula. *Journal of Glaciology*, **55**, 400-410.

GLASSER, N.F., SCAMBOS, T.A., BOHLANDER, J.A., TRUFFER, M., PETTIT, E.C. & DAVIES, B.J. 2011. From ice-shelf tributary to tidewater glacier: continued rapid glacier recession, acceleration and thinning of Röhss Glacier following the 1995 collapse of the Prince Gustav Ice Shelf on the Antarctic Peninsula. *Journal of Glaciology*, **57**, 397-406.

GOLLEDGE, N.R. 2007. An ice cap landsystem for palaeoglaciological reconstructions: characterizing the Younger Dryas in western Scotland. *Quaternary Science Reviews*, **26**, 213-229.

GOODFELLOW, B.W., FREDIN, O., DERRON, M.-H., & STROEVEN, A.P., 2008. Weathering processes and Quaternary origin of an alpine blockfield in Arctic Sweden. *Boreas*, **38**, 379-398.

GRANT, K.L., STOKES, C.R. & EVANS, I.S. 2009. Identification and characteristics of surge-type glaciers on Novaya Zemlya, Russian Arctic. *Journal of Glaciology*, **55**, 960-972.

HAEBERLI, W. 2005. Investigating glacier-permafrost relationships in high-mountain areas: historical background, selected examples and research needs. In: HARRIS, C. & MURTON, J.B. 2005. *Cryospheric systems: glaciers and permafrost.* Geological Society, London, Special Publications, **242**, 29-37.

HALL, A.M. & GLASSER, N.F. 2003. Reconstructing the basal thermal regime of an ice stream in a landscape of selective linear erosion: Glen Avon, Cairngorm Mountains, Scotland. *Boreas*, **32**, 191-207.

HALL, B.L. & DENTON, G.H. 2005. Surficial geology and geomorphology of eastern and central Wright Valley, Antarctica. *Geomorphology*, **64**, 25-65.

HAMBREY, M.J. & DOWDESWELL, J.A. 1994. Flow regime of the Lambert Glacier-Amery Ice Shelf system, Antarctica: structural evidence from LANDSAT imagery. *Journal of Glaciology*, **20**.

HAMBREY, M.J., & HUDDART, D., 1995. Englacial and proglacial tectonic processes at the snout of a thermally complex glacier in Svalbard. *Journal of Quaternary Science, **10**,* 313-326.

HAMBREY, M.J. & LAWSON, W. 2000. Structural styles and deformation fields in glaciers: a review. *In* MALTMAN, A.J., HUBBARD, B. & HAMBREY, M.J. (eds) *Deformation of Glacial Materials,* Geological Society of London, Special Publication, **176**, London, 59-83.

HAMBREY, M.J. & SMELLIE, J.L. 2006. Distribution, lithofacies and environmental context of Neogene glacial sequences on James Ross and Vega Islands, Antarctic Peninsula. *In* FRANCIS, E.A., PIRRIE, D. & CRAME, J.A. (eds)

Cretaceous-Tertiary High-Latitude Palaeoenvironments, James Ross Basin, Antarctica, Geological Society of London, Special Publication, **258**, London, 187-200.

HAMBREY, M.J. & FITZSIMONS, S.J. 2010. Development of sediment-landform associations at cold glacier margins, Dry Valleys, Antarctica. *Sedimentology*, **57**, 857-882.

HAMBREY, M.J., HUDDART, D., BENNETT, M.R., & GLASSER, N.F., 1997. Genesis of 'hummocky moraines' by thrusting in glacier ice: evidence from Svalbard and Britain. *Journal of the Geological Society, **154**,* 623-632.

HAMBREY, M.J., BENNETT, M.R., DOWDESWELL, J.A., GLASSER, N.F. & HUDDART, D. 1999. Debris entrainment and transfer in polythermal valley glaciers. *Journal of Glaciology*, **45**, 69-86.

HAMBREY, M.J., MURRAY, T., GLASSER, N.F., HUBBARD, A., HUBBARD, B., STUART, G., HANSEN, S. & KOHLER, J. 2005. Structure and changing dynamics of a polythermal glacier on a centennial timescale: Midre Lovénbreen, Svalbard. *Journal of Geophysical Research*, **110**, 1-19.

HAMBREY, M.J., SMELLIE, J.L., NELSON, A.E. & JOHNSON, J.S. 2008. Late Cenozoic glacier-volcano interaction on James Ross Island and adjacent areas, Antarctic Peninsula region. *Geological Society of America Bulletin*, **120**, 709-731.

HAMILTON, S.J. & WHALLEY, B.W. 1995. Rock glacier nomenclature: A re-assessment. *Geomorphology*, **14**, 73-80.

HARRIS, C. 2007. Periglacial Landforms: Slope Deposits and Forms. In Scott, A.E. (ed) *Encyclopedia of Quaternary Science,* Oxford: Elsevier, 2207-2217.

HARRIS, C. & MURTON, J.B. 2005. Interactions between glaciers and permafrost: an introduction. In: HARRIS, C. & MURTON, J.B. 2005. *Cryospheric systems: glaciers and permafrost.* Geological Society, London, Special Publications, **242**, 1-9.

HARRY, D.G. 1988. Ground ice and permafrost. In Clark, M.J. (ed) *Advances in periglacial geomorphology,* Chichester: Wiley-Interscience, 113-150.

HÄTTESTRAND, C. & STROEVEN, A.P. 2002. A relict landscape in the centre of Fennoscandian glaciation: Geomorphological evidence of minimal Quaternary glacial erosion. *Geomorphology*, **44**, 127-143.

HEROY, D.C. & ANDERSON, J.B. 2005. Ice-sheet extent of the Antarctic Peninsula region during the Last Glacial Maximum (LGM) - Insights from glacial geomorphology. *GSA Bulletin*, **117**, 1497-1512.

HEROY, D.C. & ANDERSON, J.B. 2007. Radiocarbon constraints on Antarctic Peninsula Ice Sheet retreat following the Last Glacial Maximum (LGM). *Quaternary Science Reviews*, **26**, 3286-3297.

HIGGINS, S.M., DENTON, G.H. & HENDY, C.H. 2000. Glacial Geomorphology of Bonney Drift, Taylor Valley, Antarctica. *Geografiska Annaler. Series A, Physical Geography*, **82**, 365-389.

HJORT, C., INGÓLFSSON, Ó., MÖLLER, P. & LIRIO, J.M. 1997. Holocene glacial history and sea-level changes on James Ross Island, Antarctic Peninsula. *Journal of Quaternary Science*, **12**, 259-273.

HJORT, C., INGÓLFSSON, Ó., BENTLEY, M.J. & BJÖRCK, S. 2003. The Late Pleistocene and Holocene glacial and climate history of the Antarctic Peninsula region as documented by the land and sediment records - a review. *In* DOMACK, E.W., LEVENTER, A., BURNETT, A., BINDSCHADLER, R., CONVEY, P. & KIRBY, M. (eds) *Antarctic Peninsula climate variability: historical and palaeoenvironmental perspectives,* Antarctic Research Series, **79**, American Geophysical Union, Washington, 95-102.

HUBBARD, B. & SHARP, M. 1995. Basal ice facies and their formation in the Western Alps. *Arctic and Alpine Research*, **27**, 301-310.

HUBBARD, B., COOK, S. & COULSON, H. 2009. Basal ice facies: a review and unifying approach. *Quaternary Science Reviews*, **28**, 1956-1969.

HUGHES, T.J. 1981. Numerical reconstruction of palaeo-ice sheets. *In* DENTON, G.H. & HUGHES, T.J. (eds) *The last great ice sheets,* John Wiley & Sons, New York, 221-261.

HUGHES, T.J. 1995. Ice sheet modelling and the reconstructions of former ice sheets from Geo(morpho)logical field data. In MENZIES, J. (ED) *Modern Glacial Environments - Processes, dynamics and sediments,* Butterworth-Heinemann Ltd, Oxford, 77-99.

HUMLUM, O. 1998. The climatic significance of rock glaciers. *Permafrost and Periglacial Processes*, **9**, 375-395.

HUMLUM, O. 2000. The geomorphic significance of rock glaciers: estimates of rock glacier debris volumes and headwall recession rates in West Greenland. *Geomorphology*, **35**, 41-67.

INESON, J.R., CRAME, J.A. & THOMSON, M.R.A. 1986. Lithostratigraphy of the Cretaceous Strata of West James Ross Island, Antarctica. *Cretaceous Research*, **7**, 141-159.

INGÓLFSSON, Ó. & HJORT, C. 2002. Glacial history of the Antarctic Peninsula since the Last Glacial Maximum - a synthesis. *Polar Research*, **21**, 227-234.

INGÓLFSSON, Ó., HJORT, C., BJÖRCK, S. & SMITH, L.R.I. 1992. Late Pleistocene and Holocene glacial history of James Ross Island, Antarctic Peninsula. *Boreas*, **21**, 209-222.

JACOBS, S.S., JENKINS, A., GIULIVI, C.F. & DUTRIEUX, P. 2011. Stronger ocean circulation and increased melting under Pine Island Glacier ice shelf. *Nature Geoscience*, **4**, 519-523.

JOHNSON, J.S. & SMELLIE, J.L. 2007. Zeolite compositions as proxies for eruptive palaeoenvironment. *Geochemistry, Geophysics, Geosystems,* **8**, doi: 10.1029/2006GC001450.

JOHNSON, J.S., SMELLIE, J.L., NELSON, A.E. & STUART, F.M. 2009. History of the Antarctic Peninsula Ice Sheet since the early Pliocene–Evidence from cosmogenic dating of Pliocene lavas on James Ross Island, Antarctica. *Global and Planetary Change*, **69**, 205-213.

JOHNSON, J.S., BENTLEY, M.J., ROBERTS, S.J., BINNEY, S.A. & FREEMAN, S.P.H.T. 2011. Holocene deglacial history of the north east Antarctic Peninsula - a review and new chronological constraints. *Quaternary Science Reviews*, **30**, 27-28.

JONES, A.P., TUCKER, M.E. & HART, J.K. 1999. *The description and analysis of Quaternary stratigraphic field sections. Technical Guide No. 7.* Cambridge: Quaternary Research Association. 293 pp.

JONKERS, H.A., LIRIO, J.M., DEL VALLE, R.A. & KELLY, S.P. 2002. Age and environment of Miocene - Pliocene glaciomarine deposits, James Ross Island, Antarctica. *Geological Magazine*, **139**, 577-594.

KING, J.C., TURNER, J., MARSHALL, G.J., CONNELLY, W.M. & LACHLAN-COPE, T.A. 2003. Antarctic Peninsula climate variability and its causes as revealed by analysis of instrumental records. *In* DOMACK, E.W., LEVENTER, A., BURNETT, A., BINDSCHADLER, R., CONVEY, P. & KIRBY, M. (eds) *Antarctic Peninsula climate variability: historical and palaeoenvironmental perspectives,* Antarctic Research Series, **79**, American Geophysical Union, Washington, 17-30.

KJÆR, K.H., KORSGAARD, N.J. & SCHOMACKER, A. 2008. Impact of multiple glacier surges - a geomorphological map from Brúarjökull, East Iceland. *Journal of Maps*, 5-20.

KJÆR, K.H. & KRÜGER, J. 2001. The final phase of dead-ice moraine development: processes and sediment architecture, Kötlujökull, Iceland. *Sedimentology*, **48**, 935-952.

KLEMAN, J. & GLASSER, N.F. 2007. The subglacial thermal organisation (STO) of ice sheets. *Quaternary Science Reviews*, **26**, 585-597.

KLEMAN, J., HÄTTESTRAND, C. & CLARHÄLL, A. 1999. Zooming in on frozen-bed patches: scale-dependent controls on Fennoscandian ice sheet basal thermal zonation. *Annals of Glaciology*, **28**, 189-194.

KLINT, K.E.S., RICHARDT, N. & KRÜGER, J. 2011. 9 Evidence for subglacial deformation and deposition during a complete advance-stagnation cycle of Kötlujökull, Iceland - a case study. *In* SCHOMACKER, A., KRÜGER, J. & KJÆR, K., H. (eds) *The Mýrdalsjökull Ice Cap, Iceland,* Elsevier, Amsterdam, 145-158.

KNIGHT, J. 2008. The environmental significance of ventifacts: A critical review. *Earth-Science Reviews*, **86**, 89-105.

KNIGHT, P.G., PATTERSON, C.J., WALLER, R.I., JONES, A.P. & ROBINSON, Z.P. 2000. Preservation of basal-ice sediment texture in ice-sheet moraines. *Quaternary Science Reviews*, **19**, 1255-1258.

KONRAD, S.K., HUMPHREY, N.F., STEIG, E.J., CLARK, D.H., POTTER, N. & PFEFFER, W.T. 1999. Rock glacier dynamics and paleoclimatic implications. *Geology*, **27**, 1131-1134.

KOŠLER, J., MAGNA, T., MLČOCH, B., MIXA, P., NÝVLT, D. & HOLUB, F.V. 2009. Combined Sr, Nd, Pb and Li isotope geochemistry of alkaline lavas from northern James Ross Island (Antarctic Peninsula) and implications for back-arc magma formation. *Chemical Geology*, **258**, 207-218.

KRÜGER, J., KJÆR, K.H. & SCHOMACKER, A. 2010. Dead-Ice Environments: A Landsystems Model for a Debris-Charged, Stagnant Lowland Glacier Margin, Kötlujökull. *In* SCHOMACKER, A., KRÜGER, J. & KJÆR, K., H. (eds) *Developments in Quaternary Science,* Elsevier, Amsterdam, 105-126.

LAITY, J. 2008. *Deserts and desert environments*. Chichester: Wiley-Blackwell. 342 pp.

LÁSKA, K., PROSEK, P. & BUDIK, L. 2010. Seasonal variation of air temperature at the Mendel Station, James Ross Island, in the period of 2006-2006. *Geophysical Research Abstracts*, **12**, EGU2010-3880.

LÁSKA, K., NÝVLT, D., ENGEL, Z., & KOPAČKOVÁ, V., 2011. Meteorological data and mass balance measurements on Davies Dome and Whisky Glacier in 2006-2010, James Ross Island, Antarctica. *Geophysical Research Abstracts*, **13**, EGU2011-4858.

LLOYD DAVIES, M.T., ATKINS, C.B., VAN DER MEER, J.J.M., BARRETT, P.J. & HICOCK, S.R. 2009. Evidence for cold-based glacial activity in the Allan Hills, Antarctica. *Quaternary Science Reviews*, **28**, 3124-3137.

LØNNE, I. & LYSÅ, A. 2005. Deglaciation dynamics following the Little Ice Age on Svalbard: Implications for shaping of landscapes at high latitudes. *Geomorphology*, **72**, 300-319.

LUKAS, S., NICHOLSON, L.I. & HUMLUM, O. 2007. Comment on Lønne and Lyså (2005): "Deglaciation dynamics following the Little Ice Age on Svalbard: Implications for shaping of landscapes at high latitudes", Geomorphology 72, 300-319. *Geomorphology*, **84**, 145-149.

LUNDQVIST, J., LILLIESKOLD, M. & OSTMARK, K. 1995. Glacial and periglacial deposits of the Tumbledown Cliffs area, James Ross Island, West Antarctica. *Geomorphology*, **11**, 205-214.

MARTIN, P.J. & PEEL, D.A. 1978. The spatial distribution of 10 m temperatures in the Antarctic Peninsula. *Journal of Glaciology*, **20**, 311-317.

MATSUOKA, N. 1995. Rock weathering processes and landform development in the Sør Rondane Mountains, Antarctica. *Geomorphology*, **12**, 323-339.

MATHEWS, W.H. & MACKAY, J.R. 1960. Deformation of soils by glacier ice and the influence of pore pressure and permafrost. *Royal Society of Canada Transactions,* LIX, Series III, Section 4, 27-36.

MAYEWSKI, P.A., MEREDITH, M.P., SUMMERHAYES, C.P., TURNER, J., WORBY, A., BARRETT, P.J., CASASSA, G., BERTLER, N.A.N., BRACEGIRDLE, T., NAVEIRA GARABATO, A.C., BROMWICH, D., CAMPELL, H., HAMILTON, G.S., LYONS, W.B., MAASCH, K.A., AOKI, S., XIAO, C. & VAN OMMEN, T. 2009. State of the Antarctic and Southern Ocean climate system. *Reviews of Geophysics*, **47**, 1-38.

MCLEOD, M., BOCKHEIM, J.G. & BALKS, M.R. 2008. Glacial geomorphology, soil development and permafrost features in central-upper Wright Valley, Antarctica. *Geoderma*, **144**, 93-103.

MIALL, A.D. 1977. A review of the braided river depositional environment. *Earth Science Reviews*, **13**, 1-62.

MURRAY, T., STROZZI, T., LUCKMAN, A., PRITCHARD, H. & JISKOOT, H. 2002. Ice dynamics during a surge of Sortebrae, East Greenland. *Annals of Glaciology*, **34**, 323-329.

MURRAY, T., STUART, G.W., MILLER, P.J., WOODWARD, J., SMITH, A.M., PORTER, P.R. & JISKOOT, H. 2000. Glacier surge propagation by thermal evolution at the bed. *Journal of Geophysical Research*, **105**, 13491-13507.

MURTON, J. 2007. Periglacial Landforms, Rock Forms: Rock Weathering. *In* SCOTT, A.E. (ed) *Encyclopedia of Quaternary Science,* Elsevier, Oxford, 2249-2256.

NASA 2004. Air Temperature Conditions and Climatic-Geomorphological Characteristics of James Ross Island, Antarctic Peninsula *Entry ID: CDA_AR_GEO_J.ROSS_CLIMATOLOGY,* Data Centre: Centro de Datos Antarcticos, Argentina: Antarctic Master Directory, http://gcmd.nasa.gov/KeywordSearch/Metadata.do?Portal=amd&KeywordPath=Parameters|LAND+SURFACE|SOILS|PERMAFROST&OrigMetadataNode=GCMD&EntryId=CDA_AR_GEO_J.ROSS_CLIMATOLOGY&MetadataView=Full&MetadataType=0&lbnode=mdlb1.

NELSON, A.E., SMELLIE, J.L., HAMBREY, M.J., WILLIAMS, M., VAUTRAVERS, M., SALZMANN, U., MCARTHUR, J.M. & REGELOUS, M. 2009. Neogene glacigenic debris flows on James Ross Island, northern Antarctic Peninsula, and their implications for regional climate history. *Quaternary Science Reviews*, **28**, 3138-3160.

NELSON, P.H.H. 1975. The James Ross Island Volcanic Group of north-east Graham Land. *British Antarctic Survey Scientific Reports*, **54**, 1-62.

NÝVLT, D., KOŠLER, J., MLČOCH, B., MIXA, P., LISÁ, L., BUBÎK, M. & HENDRIKS, B.W.H. 2011. The Mendel Formation: Evidence for Late Miocene climatic cycllicity at the northern tip of the Antarctic Peninsula. *Palaeogeography Palaeoclimatology Palaeoecology*, **299**, 363-384.

Ó COFAIGH, C., DOWDESWELL, J.A. & PUDSEY, C.J. 2001. Late Quaternary Iceberg Rafting along the Antarctic Peninsula Continental Rise and in the Weddell and Scotia Seas. *Quaternary Research*, **56**, 308-321.

Ó COFAIGH, C., EVANS, D.J.A. & ENGLAND, J.H. 2003. Ice-marginal terrestrial landsystems: sub-polar glacier margins of the Canadian and Greenland High Arctic. *In* EVANS, D.J.A. (ed) *Glacier Landsystems,* Arnold, London, 44-64.

Ó COFAIGH, C., LEMMEN, D.S., EVANS, D.J.A. & BEDNARSKI, J. 1999. Glacial landform-sediment assemblages in the Canadian High Arctic and their implications for late Quaternary glaciation. *Annals of Glaciology*, **28**, 195-201.

ØSTREM, G. 1964. Ice-cored moraines in Scandinavia. *Geografiska Annaler*, **46**, 282-337.

ØSTREM, G. 1971. Rock glaciers and ice-cored moraines, a reply to D. Barsch. *Geografiska Annaler. Series A, Physical Geography*, **53**, 207-213.

PHILLIPS, W.M., HALL, A.M., MOTTRAM, R., FIFIELD, L.K. & SUGDEN, D.E. 2006. Cosmogenic ^{10}Be and ^{26}Al exposure ages of tors and erratics, Cairngorm Mountains, Scotland: Timescales for the development of a classic landscape of selective linear glacial erosion. *Geomorphology*, **73**, 222-245.

PIRRIE, D., CRAME, J.A., RIDING, J.B., BUTCHER, A.R. & TAYLOR, P.D. 1997. Miocene glaciomarine sedimentation in the northern Antarctic Peninsula region: the stratigraphy and sedimentology of the Hobbs Glacier Formation, James Ross Island. *Geological Magazine*, **134**, 745-762.

POWERS, M.C. 1953. A new roundness scale for sedimentary particles. *Journal of Sedimentary Petrology*, **23**, 117-119.

PUDSEY, C.J. & EVANS, J. 2001. First survey of Antarctic sub-ice shelf sediments reveals Mid-Holocene ice shelf retreat. *Geology*, **29**, 787-790.

RABASSA, J. 1983. Stratigraphy of the glacigenic deposits in Northern James Ross Island, Antarctic Peninsula. *INQUA Symposium on the Genesis and Lithology of Quaternary Deposits*, 329-339.

RABASSA, J. 1987. Drumlins and Drumlinoid forms in northern James Ross Island, Antarctic Peninsula. *In* MENZIES, J. & ROSE, J. (eds) *Drumlin Symposium*, Balkema, Rotterdam, 267-288.

RABASSA, J., SKVARCA, P., BERTANI, L. & MAZZONI, E. 1982. Glacier inventory of James Ross and Vega Islands, Antarctic Peninsula. *Annals of Glaciology*, **3**, 260-264.

REA, B. 2007. Periglacial Landforms, Rockforms: Blockfields (Felsenmeer). *In* SCOTT, A.E. (ed) *Encyclopedia of Quaternary Science,* Elsevier, Oxford, 2225-2236.

REINARDY, B.T.I., PUDSEY, C.J., HILLENBRAND, C.-D., MURRAY, T. & EVANS, J. 2009. Contrasting sources for glacial and interglacial shelf sediments used to interpret changing ice flow directions in the Larsen Basin, Northern Antarctic Peninsula. *Marine Geology*, **266**, 156-171.

RILEY, T.R., FLOWERDEW, M.J. & HASELWIMMER, C.E. 2011. Geological map of Eastern Graham Land, Antarctic Peninsula (1:625 000 scale). *BAS GEOMAP 2 Series, Sheet 1,* Cambridge, UK: British Antarctic Survey.

RIPPIN, D.M., CARRIVICK, J.L., & WILLIAMS, C., 2011. Evidence towards a thermal lag in the response of Kårsglaciären, northern Sweden, to climate change. *Journal of Glaciology, **57**,* 895-903.

ROBERTS, S.J., HODGSON, D.A., STERKEN, M., WHITEHOUSE, P.L., VERLEYEN, E., VYVERMAN, W., SABBE, K., BALBO, A., BENTLEY, M.J. AND MORETON, S.G. 2011. Geological constraints on glacio-isostatic adjustment models of relative sea-level change during deglaciation of Prince Gustav Channel, Antarctic Peninsula. *Quaternary Science Reviews*, **30**, 3603-3617.

SCHAFER, J.M., BAUR, H., DENTON, G.H., IVY-OCHS, S., MARCHANT, D.R., SCHLUCHTER, C., & WIELER, R. 2000. The oldest ice on Earth in Beacon Valley, Antarctica: new evidence from surface exposure dating. *Earth and Planetary Science Letters,* **179**, 91-99.

SCHOMACKER, A. 2008. What controls dead-ice melting under different climate conditions? A discussion. *Earth-Science Reviews*, **90**, 103-113.

SCHOMACKER, A. & KJÆR, K.H. 2007. Origin and de-icing of multiple generations of ice-cored moraines at Brúarjökull, Iceland. *Boreas*, **36**, 411-425.

SCHOMACKER, A. & KJÆR, K.H. 2008. Quantification of dead-ice melting in ice-cored moraines at the high-Arctic glacier Holmströmbreen, Svalbard. *Boreas*, **37**, 211-225.

SERRANO, E. & LÓPEZ-MARTÍNEZ, J. 2000. Rock glaciers in the South Shetland Islands, Western Antarctica. *Geomorphology*, **35**, 145-162.

SHARP, M.J., JOUZEL, J., HUBBARD, B. & LAWSON, W. 1994. The character, structure and origin of the basal ice layer of a surge-type glacier. *Journal of Glaciology*, **40**, 327-340.

SIEGERT, M.J. 2009. Numerical modelling of the Antarctic Ice Sheet. *In* SIEGERT, M.J. & FLORINDO, F. (eds) *Antarctic Climate Evolution,* Elsevier, Rotterdam, 235-256.

SIEGERT, M.J. & DOWDESWELL, J.A. 2004. Numerical reconstructions of the Eurasian Ice Sheet and climate during the Late Weichselian. *Quaternary Science Reviews*, **23**, 1273-1283.

SMELLIE, J.L., HAYWOOD, A.M., HILLENBRAND, C.-D., LUNT, D.J. & VALDES, P.J. 2009. Nature of the Antarctic Peninsula Ice Sheet during the Pliocene: Geological evidence and modelling results compared. *Earth-Science Reviews*, **94**, 79-94.

SMELLIE, J.L., JOHNSON, J.S., MCINTOSH, W.C., ESSER, R., GUDMUNDSSON, M.T., HAMBREY, M.J. & VAN WYK DE VRIES, B. 2008. Six million years of glacial history recorded in volcanic lithofacies of the James Ross Island Volcanic Group, Antarctic Peninsula. *Palaeogeography, Palaeoclimatology, Palaeoecology*, **260**, 122-148.

SMELLIE, J.L., MCARTHUR, J.M., MCINTOSH, W.C. & ESSER, R. 2006. Late Neogene interglacial events in the James Ross Island region, northern Antarctic Peninsula, dated by Ar/Ar and Sr-isotope stratigraphy. *Palaeogeography, Palaeoclimatology, Palaeoecology*, **242**, 169-187.

SONE, T., FUKUI, K., STRELIN, J.A., TORIELLI, C.A. & MORI, J. 2007. Glacier lake outburst flood on James Ross Island, Antarctic Peninsula region. *Polish Polar Research*, **28**, 3-12.

SPEDDING, N. & EVANS, D.J.A. 2002. Sediments and landforms at Kviarjokull, southeast Iceland: a reappraisal of the glaciated valley landsystem. *Sedimentary Geology*, **149**, 21-42.

STOKES, C.R. & CLARK, C.D. 1999. Geomorphological criteria for identifying Pleistocene ice streams. *Annals of Glaciology*, **28**, 67-74.

STOKES, C.R. & CLARK, C.D. 2001. Palaeo-ice streams. *Quaternary Science Reviews*, **20**, 1437-1457.

STRELIN, J.A. & MALAGNINO, E.C. 1992. Geomorfologìa de la Isla James Ross. *Geologia de la Isla James Ross,* Buenos Aires: Instituto Antàrctico Argentino, 7-36.

STRELIN, J.A. & SONE, T. 1998. Rock glaciers on James Ross Island, Antarctica. *Permafrost - Seventh International Conference (Proceedings)*, **55**, 1027-1033.

STRELIN, J.A., SONE, T., MORI, J., TORIELLI, C.A. & NAKAMURA, E. 2006. New data related to Holocene landform development and climatic change from James Ross Island, Antarctic Peninsula. *In* FÜTTERER, D.K., DAMASKE, D., KLEINSCHMIDT, G., MILLER, H. & TESSENSOHN, F. (eds) *Antarctica: contributions to global Earth sciences. Proceedings of the IX International Symposium of Antarctic Earth Sciences, Potsdam, 2003,* Springer-Verlag, New York, 455-460.

STRELIN, J.A., TORIELLI, C.A., SONE, T., FUKUI, K. & MORI, J. 2007. Particularidades geneticas de glaciares de roca la Isla James Ross, Peninsula Antartica. *Revista de la Asociacion Argentina*, **62**, 627-634.

STROEVEN, A.P., FABEL, D., HÄTTESTRAND, C. & HARBOR, J. 2002. A relict landscape in the centre of Fennoscandian glaciation: cosmogenic radionuclide evidence of tors preserved through multiple glacial cycles. *Geomorphology*, **44**, 145-154.

SUGDEN, D.E., MARCHANT, D.R., POTTER, N., SOUCHEZ, R.A., DENTON, G.H., SWISHER, C.C. & TISON, J.-L.

1995. Preservation of Miocene glacier ice in East Antarctica. *Nature*, **376**, 412-414.

SUGDEN, D.E., SUMMERFIELD, M.A., DENTON, G.H., WILCH, T.I., MCINTOSH, W.C., MARCHANT, D.R. & RUTFORD, R.H. 1999. Landscape development in the Royal Society Range, southern Victoria Land, Antarctica: stability since the mid-Miocene. *Geomorphology*, **28**, 181-200.

THORN, C.E. 1988. Nivation: a geomorphic chimera. In CLARK, M.J. (ed) *Advances in periglacial geomorphology,* Chichester: Wiley-Interscience, 3-32.

TROMBOTTO, D., 2002. Inventory of fossil cryogenic forms and structures in Patagonia and the mountains of Argentina beyond the Andes. *South African Journal of Science*, **98**, 171-180.

VAN LIPZIG, N.P.M., KING, J.C., LACHLAN-COPE, T.A. & VAN DEN BROEKE, M.R. 2004. Precipitation, sublimation and snow drift in the Antarctic Peninsula region from a regional atmospheric model. *Journal of Geophysical Research*, **109**, D24106.

WADHAM, J.L. & NUTTALL, A.-M. 2003. Multiphase formation of superimposed ice during a mass-balance year at a maritime high-Arctic glacier. *Journal of Glaciology*, **48**, 545-551.

WALDEN, J.S. 2004. Particle Lithology (or mineral and geochemical analysis). *In* EVANS, D.J.A. & BENN, D.I., editors, *A practical guide to the study of glacial sediments,* Arnold, London, 145-180.

WALLER, R.I. 2001. The influence of basal processes on the dynamic behaviour of cold-based glaciers. *Quaternary International*, **86**, 117-128.

WALLER, R.I., HART, J.K. & KNIGHT, P.G. 2000. The influence of tectonic deformation on facies variability in stratified debris-rich basal ice. *Quaternary Science Reviews*, **19**, 775-786.

WALLER, R.I., MURTON, J.B. & KNIGHT, P.G. 2009. Basal glacier ice and massive ground ice: different scientists, same science? In: KNIGHT, J. & HARRISON, S. 2009. *Periglacial and paraglacial processes and environments.* The Geological Society, London, Special Publications, **320**, 57-69.

WILSON, P. 2007. Periglacial Landforms: Rock Forms. *In* SCOTT, A.E. (ed) *Encyclopedia of Quaternary Science,* Elsevier, Oxford, 2217-2225.

ŽÁK, J., SOEJONO, I., JANOUŠEK, V. &VENERA, Z. 2011. Magnetic fabric and tectonic setting of the Early to Middle Jurassic felsic dykes at Pitt Point and Mount Reece, eastern Graham Land, Antarctica. *Antarctic Science*, **in press**.

Figures

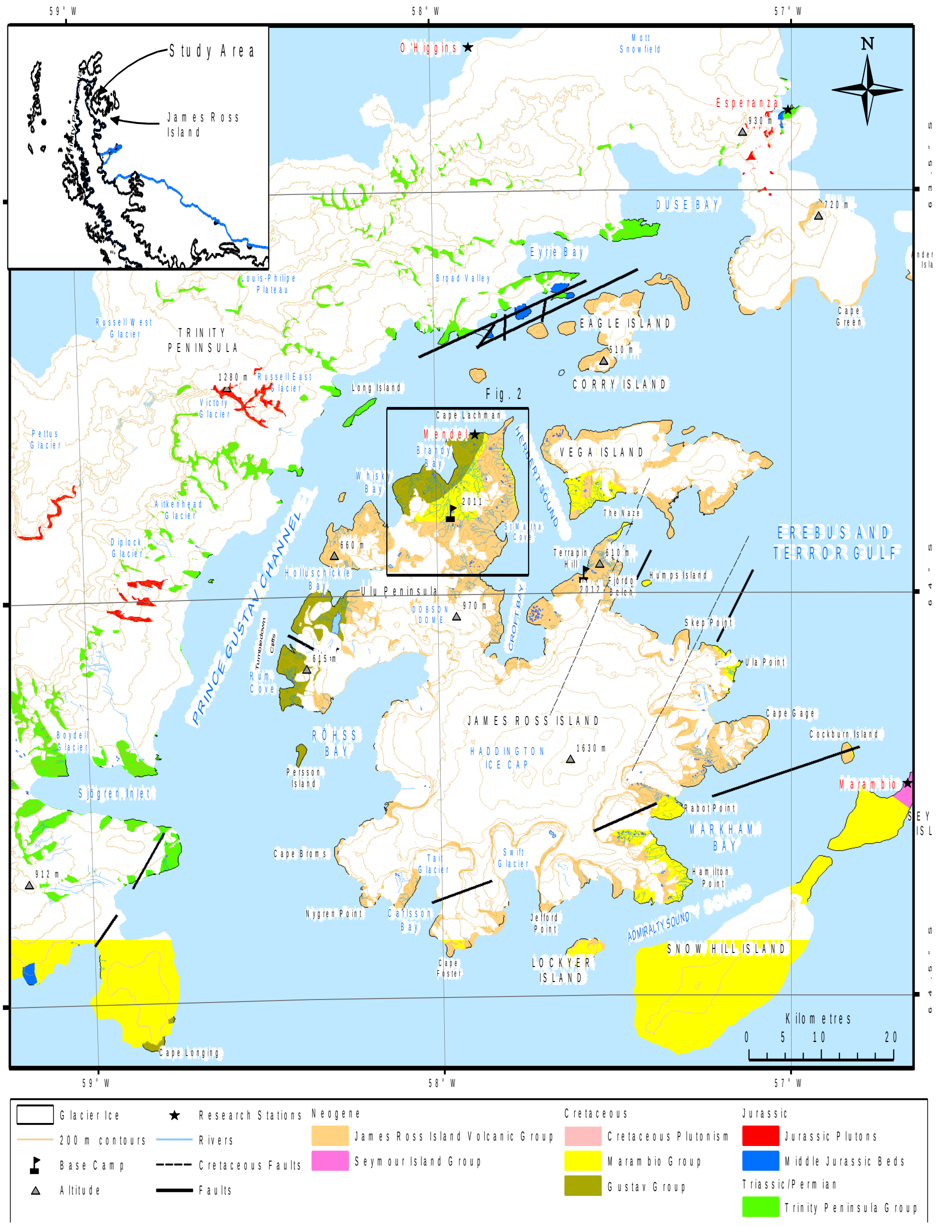

Fig. 1. James Ross Island and Ulu Peninsula, NE Antarctic Peninsula. Study region is in boxed area on main map. Inset shows the wider regional context of James Ross Island. Main map shows the location of Cretaceous, James Ross Island Volcanic Group, Trinity Peninsula Group and granite lithologies (Bibby 1966; Nelson 1975; British Antarctic Survey 2010; Riley *et al.* 2011). James Ross Island Volcanic Group: Miocene to recent basaltic lava, tuff, hyaloclastite and breccia. Seymour Island Group: Palaeogene-Eocene richly fossiliferous, shallow water, fine grained volcaniclastic sedimentary rocks. Marambio Group: Santonian-Palaeocene fossiliferous, shallow water fine grained volcaniclastic sedimentary rocks. Gustav Group: Barremian-Albian coarse grained volcaniclastic sedimentary rocks; deeper water environment. Cretaceous plutons: typically granodiorite. Jurassic plutons: granite-tonalite-quartz mononzite. Mapple, Mt Flora and Kenney Glacier formations and Botany Bay Group: mainly rhyolitic ignimbrite. Trinity Peninsula Group: Permo-Triassic siliclastic turbidite succession with interbedded basic volcanic rocks.

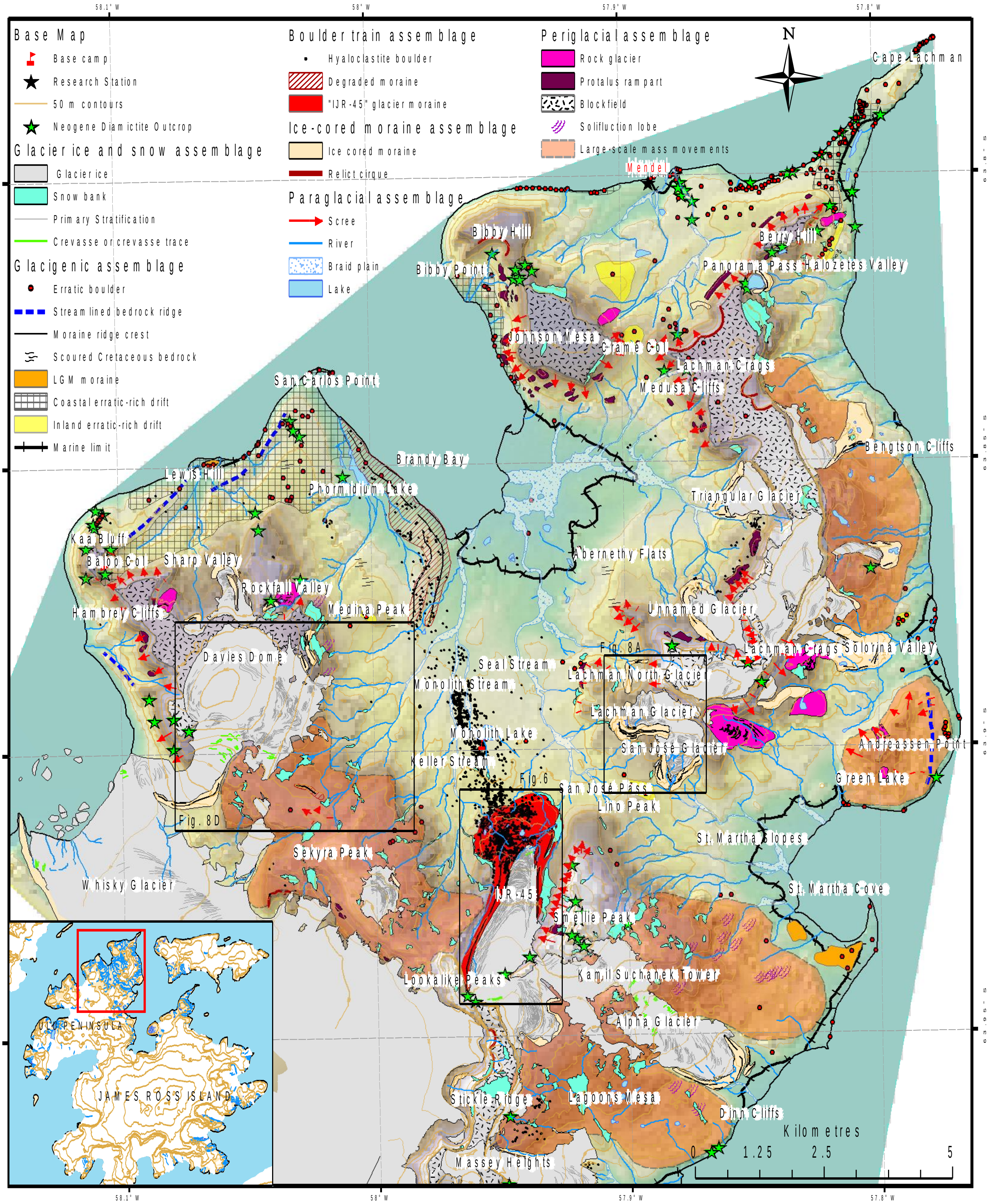

Fig. 2. Geomorphological map of northern Ulu Peninsula, showing the main features from the six sediment-landform assemblages. Overlain on the 2006 DEM and using ice, perennial snow, braid plains and rivers mapped by the Czech Geological Survey (2009). Glacier structures are mapped from aerial photographs from the year 2006.

Fig. 3. Principal characteristics of Glacier Ice and Snow Assemblage on Ulu Peninsula. A. Lachman (left) and San José (right) glaciers, with stratification. Note large ice-cored moraines. B. “Unnamed Glacier”, with supraglacial debris falling onto the glacier head from scree (arrowed, “b”) and emerging near the snout (arrowed, “a”). C. Stagnant and down-wasting ice mass with prominent ice-cored moraines. View downwards from the top of Lachman Crags, looking east. Arrow indicates an ice scar with stratified ice. D. Stratification in San José glacier (arrowed).

Fig. 4. Glacial drifts on Ulu Peninsula. Drift sheets in photographs A to G were emplaced during the LGM. A. Erratic-poor drift. Lone striated, faceted granite erratic with red staining in a region otherwise devoid of erratics in Solarina Valley. The basalt-rich drift is a sandy gravel with scattered cobbles with an *a*-axis of up to 30 cm. The gravel is almost 100 % angular to subangular basalt. B. Erratic-poor drift. Lone granite erratic in the forefield of “IJR-45”,

where it rests as an isolated boulder on an otherwise entirely basaltic surficial drift. Basalt boulders can be seen protruding through the glacial drift surface. The boulder appears to be a ventifact. “IJR-45” moraine can be seen in the distance. C. Erratic-poor drift with broken and brecciated Cretaceous bedrock with stone stripes emanating from basalt cobbles. D. Erratic-poor drift on broken and brecciated Cretaceous bedrock with scattered basalt erratics on the surface. E. Erratic-poor drift on scoured Cretaceous bedrock with few erratics or cobbles on the surface. The different beds are clearly visible. Note the basaltic mesas in the distance (Johnson Mesa (left) and Lachman Crags). F. Coastal erratic-rich drift with numerous white granite boulders protruding through the drift at Cape Lachman. People are encircled for scale. Note the contrast in the colour of the drift with the brown surfaces with no Trinity Peninsula erratics in the distance. Numerous granite erratics are well-embedded in the surficial sediments at this location. Note the abundant granite pebbles, giving the surface a speckled white appearance. G. Erratic-rich drift on fragment of moraine behind Kaa Bluff on the edge of Prince Gustav Channel (cf. Fig. 2). Note the difference in surface texture to the smooth slopes with stone runs on the steep slopes of Kaa Bluff in the background. Note also the presence of several large granite boulders perched on the surface, whose white colour contrasts with the brown basalts that make up the majority of the surface. No stone stripes or polygons are evident on the moraine fragment. H. Boulder Train Assemblage, near Monolith Lake. Note the large hyaloclastite monoliths. Prince Gustav Channel and Trinity Peninsula in the distance.

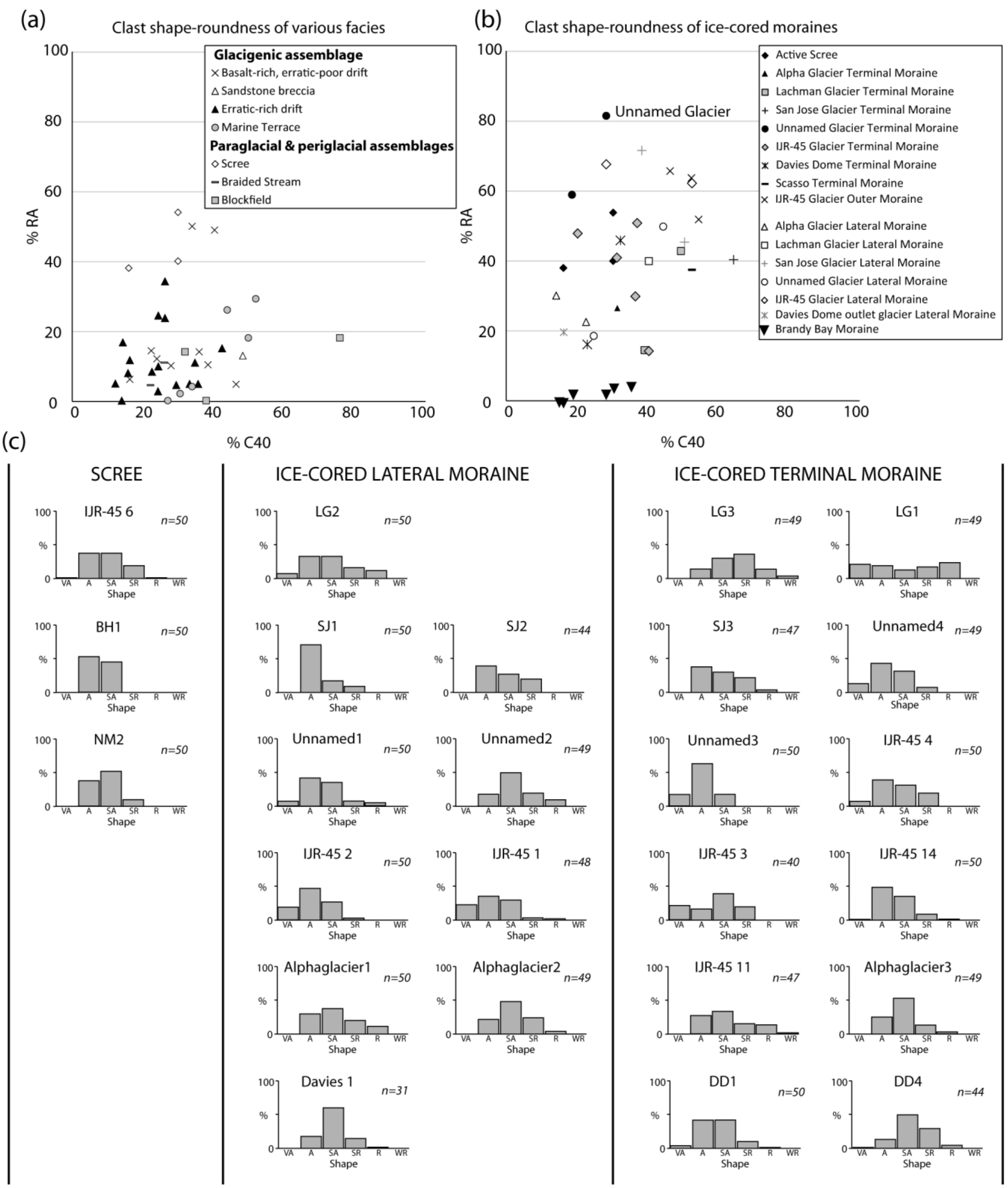

Fig. 5. C_{40} / RA plots and clast-roundness histograms of the different land elements of the sediment-landform assemblages: A. glacial drifts; B. ice-cored moraines. All shape-roundness measurements were carried out on basalt clasts. All samples show considerable modification from the original source material (scree) but there is considerable overlap between those samples with Trinity Peninsula erratics and those without, perhaps highlighting the similar transport distances for all samples; all the basalts are locally-derived and so have similar transport histories. C. Angularity histograms for ice-cored moraine samples.

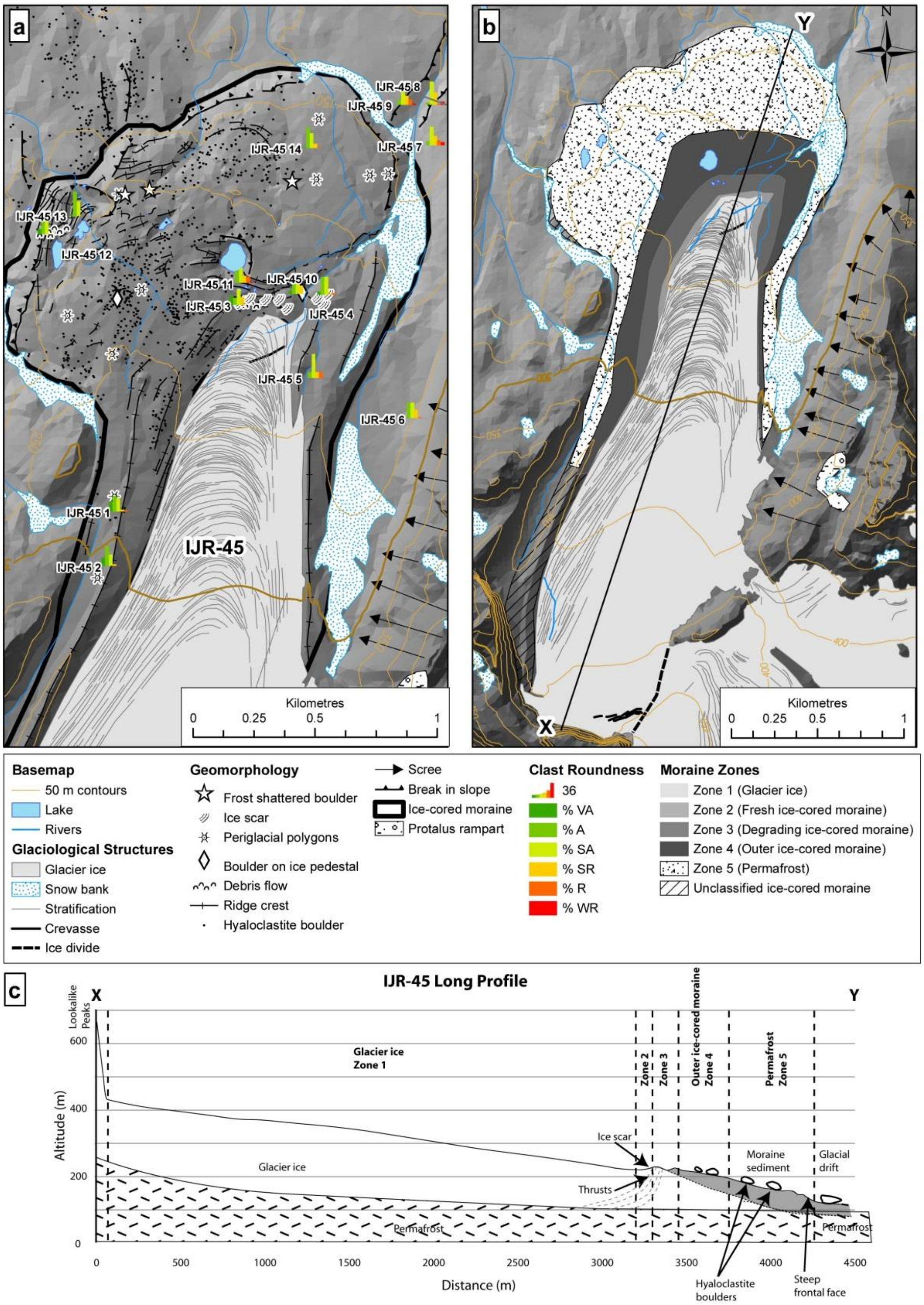

Fig. 6. Boulder train assemblage. A. Geomorphological map of “IJR-45 Glacier Moraine”, showing degradation of ice-cored moraine on “IJR-45”. Refer to Fig. 2 for regional situation. B. Landform zonation on “IJR-45 Glacier Moraine”, from fresh ice-cored moraine to an outer zone of permafrost. Refer to Table 5. C. Annotated long profile of “IJR-45”, along line XY marked on Fig. 6B. Maps are overlain on the 2006 DEM (Czech Geological Survey 2009).

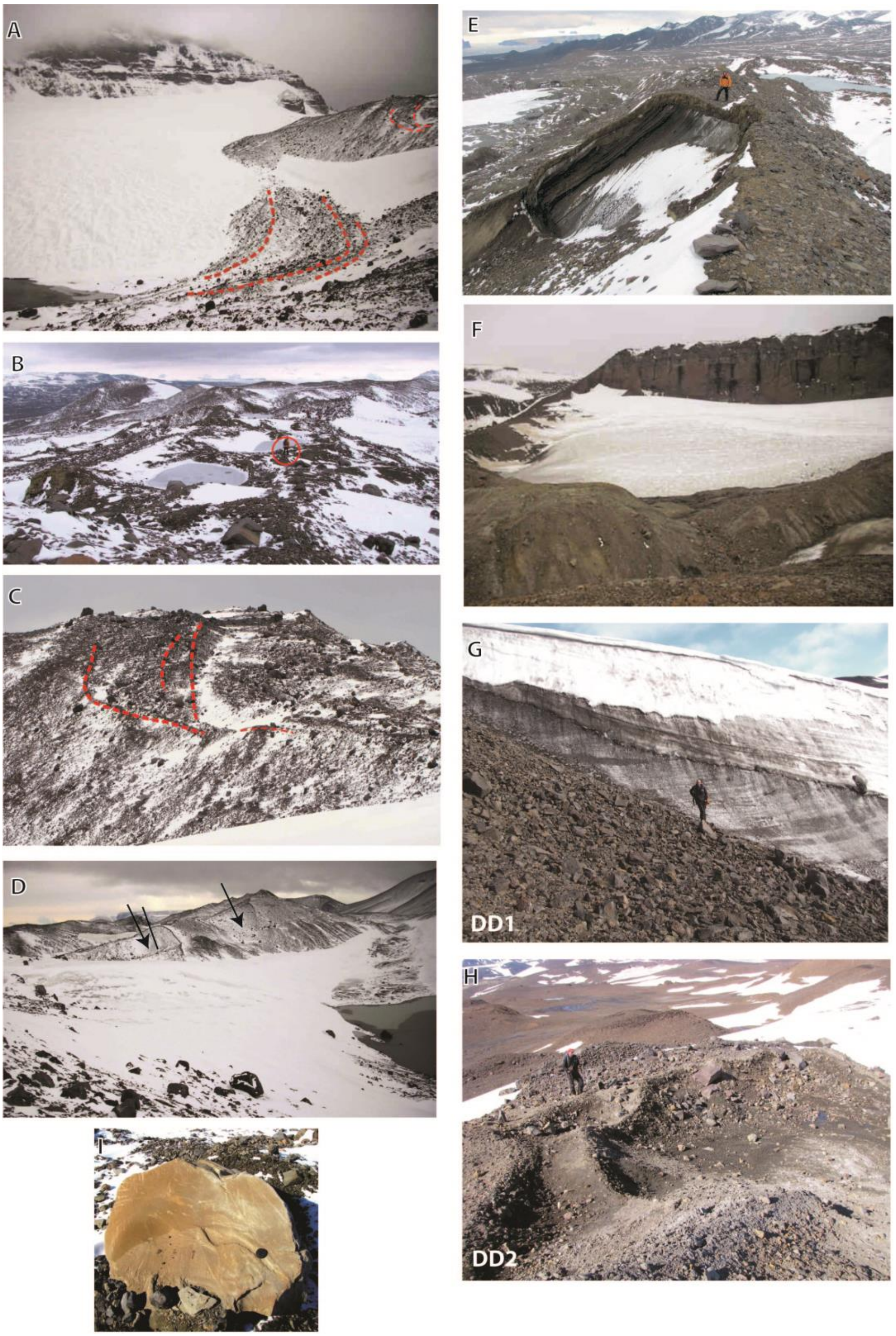

Fig. 7. Late-Holocene moraines on James Ross Island. A. Inner moraines on Lachman Glacier. B. Kettle lakes on Lachman Glacier moraine. C. Thrusts (red dashed lines) on the inner face of Lachman Glacier latero-terminal moraine. D. Ice scars (arrowed) exposed in the true right latero-terminal moraine on Lachman Glacier. E. Section 2; exposure of stratified ice in the lateral moraine on San José Glacier. F. The ice-cored moraine of Triangular Glacier. I. Striated sandstone boulder at the proximal terminal moraine of “IJR-45”. G. Sample location DD1; margin of Davies

Dome. Refer to Fig. 2 for regional situation. Samples DD1 and DD2 are in close proximity but are strikingly different. Sample DD1 is in front of an ice cliff, with ice-contact scree forming and flowing down-slope under gravity. The surface is openwork gravel and boulders. Note the unconformity within the stratified ice, which contains boulders of basalt. The stone lithologies are all angular to subangular basalt. H. Sample DD2 is characterised by chaotic mounds and ridge crests on the ice-cored moraine in front of the lower lobed margin of Davies Dome. Refer to Fig. 5C for angularity histograms. I. Striated Cretaceous sandstone boulder in the proximal terminal moraine for IJR-45. Camera lens cap for scale.

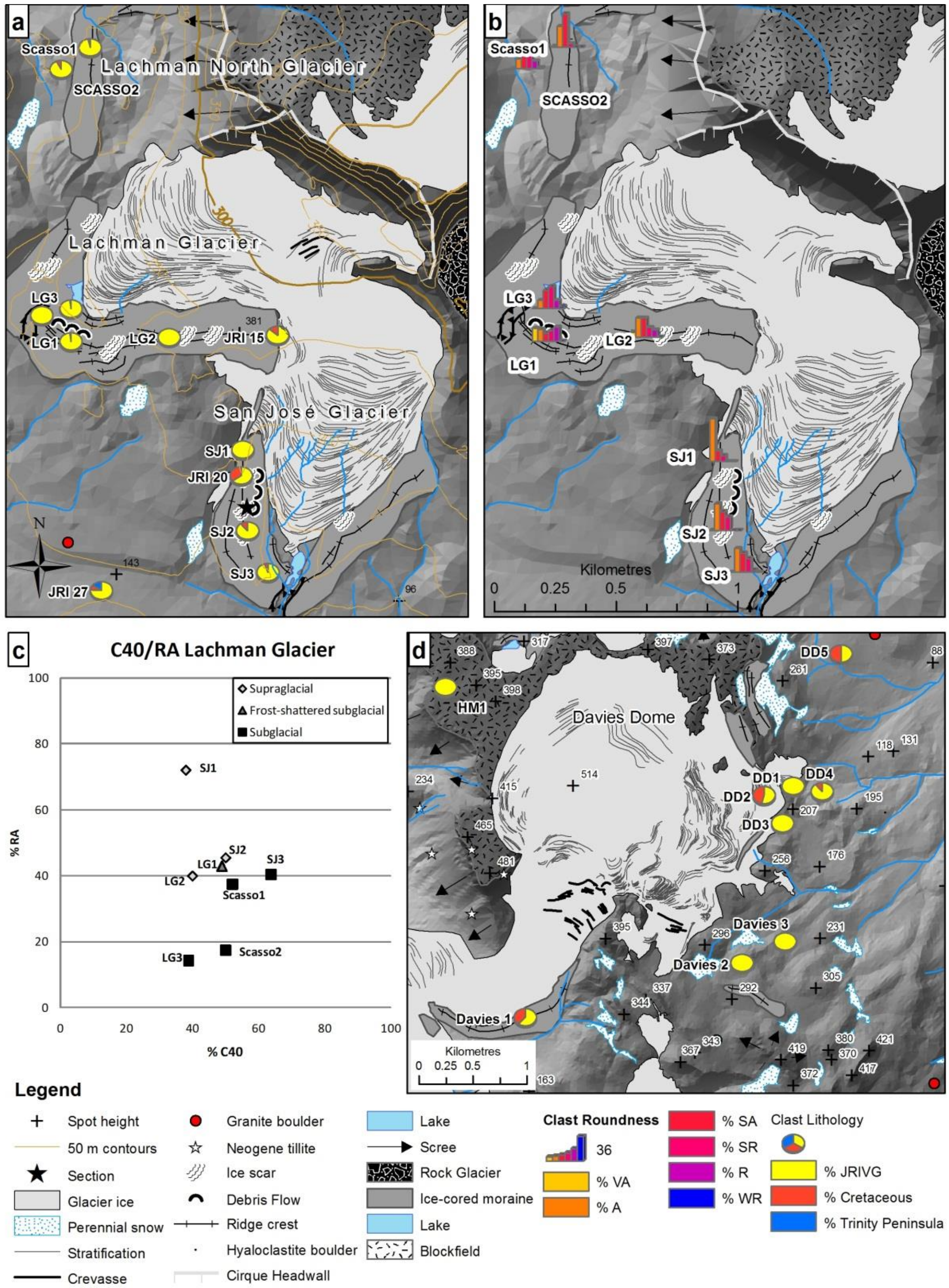

Fig. 8. Ice-cored moraine assemblage. A and B: Glaciological and geomorphological map of San José and Lachman glaciers and their associated moraines. Refer to Fig. 2. for regional situation. Note how the moraines mirror the primary stratification. Overlain on the 2006 DEM (Czech Geological Survey 2009). The lithological composition of moraine surface samples (n=50) is shown. B. Map showing roundness data of surface pebble samples (n=50). C. C_{40}/RA plot of shape-roundness data of all samples. D. Map of Davies Dome Glacier, showing sample locations DD1 and DD2.

Fig. 9. Paraglacial assemblage. A. Marine terrace at site Aber 3 site, Abernethy Flats, facing Brandy Bay. Surface is flat and featureless, with few boulders. Clasts are 100 % locally-derived basalts and hyaloclastites. Clast shape shows a high degree of clast rounding. Dashed line indicates margin of modern beach. B. Marine terrace in front of Alpha Glacier. People circled for scale Dashed line indicates margin of marine terrace. C. Idealised sketch of the marine terraces in front of Alpha Glacier. D. Bohemian Stream, draining towards Mendel Station. E. Monolith Stream, Brandy Bay. Braided stream incised through the marine terrace on Abernethy Flats, draining into Brandy Bay. Note the point bars, multiple channels and low-volume discharge. F. Wind-blown sand on snow patch below Crame Col. G. Detail of windblown sand on snow patch below Crame Col. H. Aeroxysts on a basalt boulder.

Fig. 10. Paraglacial landforms: large scale mass movements. A. Landslide below the col between Johnson Mesa and Bibby Hill. B. South side of Berry Hill. There is a large block of hyaloclastite with subaerial lava cap that has detached, tilted outwards (to right hand side) slightly and started to fall away from Berry Hill (subaerial lavas still *in situ* on Berry Hill top partly seen at left). A few smaller degraded hyaloclastite blocks can be seen in the background right hand side at a lower level. C. Berry Hill looking down the E side of Lachman Crags. The middle distance and far left are hummocky terrain underlain by multiple large mass movement blocks derived from Lachman Crags. Also visible (arrowed) is a block that has dropped a few tens of metres but is still upright - i.e. frozen in action as it detaches and begins its downslope journey. D. Schematic diagram illustrating processes involved in the emplacement of the large-scale mass movement of sections of the lava-fed deltas on James Ross Island. Instability near the margins of the delta following the removal of supporting ice or seawater is envisaged causing stress-release fracturing, with fractures potentially propagating down to intersect any fine-grained (sandy) bottomset layers in the predominantly very coarse hyaloclastite breccias. Note that, although the sandy layers probably acted as weak ductile surfaces of décollement, they are comparatively uncommon and delta flank collapses also occurred in sections lacking sandy interbeds. However, their presence and greater structural weakness relative to the enclosing hyaloclastite breccias ensures that if present they probably act preferentially as décollement surfaces. For clarity, the diagram does not illustrate the presence and potential importance of high porewater pressures beneath a subglacial and/or proglacial permafrost layer, which would reduce the effective stress of the substrate and promote lateral instability and collapse.

Fig. 11. Periglacial phenomena. A. Talus-derived rock glaciers on Andreasson Point (arrowed). B. Talus-derived rock glacier below Berry Hill. C. Protalus rampart on the eastern face of Lachman Crags (arrowed). D. Protalus ramparts below Davies Dome mesa. E. Solifluction lobes (arrowed) mantling the slopes of a hill made of hyaloclastite. Person for scale (circled).

Fig. 12. Periglacial phenomena. A. Frost-shattered basalt boulder near DD2, with the detritus moving downslope under periglacial processes. B. Nivation processes south of the neck of Cape Lachman promontory. C. Stone polygon nets, near Green Lake. D. Stone stripes with coarser basalt cobbles concentrated in the centre of the stripes, northern Brandy Bay area. E. Blockfield of basalt fragments on top of Lachman Crags mesa. F. Basalt boulder on top of Lachman Crags mesa, turned sub-vertical under freeze-thaw processes.

Fig. 13. Conceptual model illustrating the principal processes and sediment-landform assemblages in a semi-arid polar desert, based on Ulu Peninsula of James Ross Island, showing simplified geology and surficial sediments.

Fig. 14. Schematic cartoon illustrating the relative importance of various modern processes and the abundance of different products across a latitudinal transect from Northern Patagonia (northern Chile), through Tierra del Fuego (southern Chile) and James Ross Island to the Dry Valleys (Northern Victoria Land, East Antarctica). Thermal regimes change from temperate to cold-based; glacier velocities decrease southwards; meltwater is progressively abundant northwards. The shaded shapes illustrate the relative importance or abundance of a process or product, with 1 being low importance and 5 being high importance or very abundant. Sources include Trombotto (2002); Bentley *et al.* (2005); Glasser *et al.* (2009a); Hambrey & Fitzsimons (2010).